Effective dispersion in temporally fluctuating flow through a heterogeneous medium

Marco Dentz* and Jesus Carrera†

Department of Geotechnical Engineering and Geosciences, Technical University of Catalonia (UPC), Barcelona, Spain

(Received 3 June 2003; published 19 September 2003)

In this paper we investigate the effective transport of a passive solute in temporally fluctuating flow through a spatially heterogeneous medium. The Darcy equation for an incompressible fluid in the heterogeneous medium is solved with temporally fluctuating boundary conditions using perturbation theory. We distinguish between a spatial random process reflecting the medium heterogeneities and a temporal random process which models the fluctuations of the boundary conditions. By appropriately averaging over the corresponding random fields, we evaluate the second-order perturbation approximation to the time evolution of the "effective" and "ensemble" dispersion coefficients. Both quantities consist of three terms reflecting: (1) local dispersion; (2) dispersion caused by spatial heterogeneities (identical to the corresponding dispersion in steady random flow); (3) dispersion linked to the enhanced solute spreading caused by the interactions between temporal fluctuations, local dispersion, and spatial heterogeneity. The behavior of this latter contribution is complex due to the interplay of three different time scales (set by fluctuating boundary conditions, local dispersion, and advection). Temporal fluctuations of the velocity field lead to effective transverse dispersion coefficients that evolve in time to macroscopic values (i.e., independent of the local dispersion), which is consistent with observations in the field but was not predicted by theories based on steady flow. Due to their perturbative nature, the derived results are intrinsically limited to moderately fluctuating random velocity fields. However, numerical transport simulations indicate a wide range of applicability. The reported results support remediation techniques that attempt to enhance the mixing of injected reactants with contaminated ground water by temporal variations of injection and pumping rates.

DOI: 10.1103/PhysRevE.68.036310 PACS number(s): 47.55.Mh, 05.60.−k, 92.40.Kf, 02.50.Ey

I. INTRODUCTION

We investigate the transport behavior of a passive solute in an incompressible temporally fluctuating velocity field through a heterogeneous porous medium in a stochastic modeling framework. The study is motivated by the application to contaminant movement in saturated ground water aquifers, where the flow always fluctuates spatially and temporally.

It is well known that medium heterogeneities on a local scale have an important impact on the effective large scale behavior of solute transport. The dominant influence of medium heterogeneities has been studied extensively during the last two decades within a stochastic framework, e.g., Refs. [1–3]. Here we investigate the effective large scale transport behavior due to the interplay between spatial heterogeneities of the porous medium, local dispersion and time fluctuations of the flow field, as observed in realistic subsurface flows, e.g., Refs. [4–6].

The stochastic analysis of transport in steady heterogeneous ground water flow describes well the longitudinal (in direction of the mean flow) effective spreading of solute found on the field scale while the effective transverse spreading is underestimated by theoretical findings by at least one order of magnitude, e.g., Ref. [2]. One objective of this study is to systematically investigate the influence of temporal variations of the flow velocity on the transverse spreading in a typical realization of the heterogeneous medium. It was shown by Rehfeldt and Gelhar [5] that temporal fluctuations of the flow through a heterogeneous medium represent a possible source of macroscopic transverse spreading. Ackerer and Kinzelbach [7] noticed the importance of temporal fluctuations of ground water flow on the large scale transport behavior and analyzed the influence of temporally fluctuating flow in a homogeneous porous medium by random walk simulations. A similar flow and transport model has been investigated in Ref. [8]. Transport in a time-periodical heterogeneous flow field has been investigated in Ref. [9] using an effective transport framework. Exact averaging of the stochastic transport equations for time-dependent flow in a homogeneous medium was investigated in Ref. [10]. Effective macrodispersion coefficients in transient ground water flow are considered in Ref. [11].

The transport of a passive scalar in time-dependent and steady random flow fields has been frequently addressed in the physics literature in the context of turbulent diffusion and for the study of random walks in random environments, e.g., Refs. [12–23]. However, application to flow and solute transport in the subsurface displays two important features that have to be taken into account. First, the velocity field is derived from the continuity equation and Darcy's law [24] (contrary to the more frequent derivation of the incompressible velocity field from a general Gauss distributed vector potential, e.g., Refs. [16,20,21]). Second, in contrast to many models investigating transport in turbulent flow or steady random flow, e.g., Refs. [15,16,19–22], which assume a zero mean velocity, the mean flow is necessarily non-zero, which leads to qualitatively and quantitatively different transport behavior, e.g., Refs. [12,23]. Diffusion in biased random velocity fields [23,25,26] finds application also, e.g., in plasma

*Electronic address: marco.dentz@upc.es

†Electronic address: jesus.carrera@upc.es

turbulence, meteorology, or oceanography [27–29].

Neglecting compressibility is a good approximation for flow in the subsurface because the compressibility time scales tend to be much smaller than the time scales of fluctuations, e.g., Ref. [5]. The flow equation is then derived from the Darcy equation by applying the incompressibility condition for the fluid. In the approach used here, the flow field is given by the linearized solution of this flow equation [2,5] for time-fluctuating boundary conditions for the hydraulic head (pressure). The time fluctuations are not erratic and can be characterized by a short range correlation function [5] with a finite correlation time.

The objective of this work is to quantify the influence of space and time fluctuations of flow through a heterogeneous medium on the effective transport behavior of a contaminant by studying the effective center of mass velocity and effective dispersion coefficients, which are defined in one realization of the random medium by

$$u_i^R(t)=\frac{d}{dt}m_i^{(1)}(t), \tag{1}$$

$$D_{ij}^R(t)=\frac{1}{2}\frac{d}{dt}\{m_{ij}^{(2)}(t)-m_i^{(1)}(t)m_j^{(1)}(t)\}, \tag{2}$$

respectively, where the first and second moments of the concentration distribution are defined by $m_i^{(1)}(t) \equiv\int d^dx x_i c(\mathbf{x},t)$ and $m_{ij}^{(2)}(t)\equiv\int d^dx x_i x_j c(\mathbf{x},t)$.

In a stochastic model these observables are defined as averages over all typical realizations of the stochastic processes under consideration. It is essential to consider appropriately defined averages in order to assure that the chosen observables characterize the spreading of the solute in a typical realization rather than the spreading properties of the ensembles under consideration: The observables should be self-averaging. This important issue has been recognized for the transport in turbulent flow fields [30,31] as well as for the transport in time-independent random flow fields [32]. The importance of an appropriate choice of dispersion coefficients for the correct representation of reactive transport has been addressed recently [33,34].

In this context, one distinguishes between the "effective" and "ensemble" dispersion coefficients, e.g., Refs. [32,35–37], for transport in steady random flow fields. The effective dispersion coefficient is defined by the average of Eq. (2) over all typical realizations of the (spatial) random process and is a measure of spreading in any typical realization of the medium. As such, it reflects the actual spreading of the solute. The ensemble dispersion coefficient, in contrast, is derived from the ensemble averaged concentration distribution and reflects the dispersion properties of the ensemble of all realizations. As such, it reflects not only the solute spreading but also the uncertainty in the displacement of the center of mass of the solute distribution, which represents an additional (artificial) spreading effect. The difference between the effective and ensemble dispersion coefficients has been discussed quantitatively in Refs. [35,36,38,39] for the disorder-induced contributions due to a time-independent random flow field. These two dispersion coefficients converge to the same asymptotic value for times that are large compared to the dispersion time scale $\tau_D=l^2/D$, which measures the time for the dispersive transport of the solute over one correlation length scale of the medium by local dispersion D. The effective dispersion coefficient evolves on the dispersion time scale τ_D while the time evolution of the ensemble dispersion coefficient is dominated by the advection time scale $\tau_u=l/u$, which measures the time for advective transport by the mean velocity u over a typical (correlation) length scale l of the medium. For realistic aquifer situations the advection and dispersion time scales are well separated, $\tau_u\ll\tau_D$ [2].

For the time-dependent random flow field under consideration here we deal with a spatial and a temporal random process, which represent the spatial fluctuations of the heterogeneous medium and the time fluctuations of the flow boundary conditions, respectively. This causes a third time scale (namely, the correlation time of temporal fluctuations, τ) to arise. The magnitude of this scale is compared to the advection time scale by means of the Kubo number [23], defined as $\kappa\equiv\tau/\tau_u$.

A straightforward generalization of the concepts developed for steady state flow fields leads to an effective dispersion coefficient D_{ij}^{eff}, which is defined as the average of the dispersion coefficient (2) in a typical realization, over both the spatial and temporal ensembles. As for transport in a steady random flow field, this quantity characterizes the spreading in a typical realization of the spatial and temporal random ensembles. Furthermore, in analogy to transport in steady random flow, we define an "ensemble" dispersion coefficient D_{ij}^{ens} as the time ensemble average over the dispersion coefficient derived from the space ensemble averaged concentration distribution. These observables are investigated using a second-order perturbation expansion in the variance of the random flow field. As such the presented results are intrinsically limited to moderately fluctuating random velocities. As it turns out, the so defined effective and ensemble dispersion coefficients converge for times that are large compared to τ_D.

II. BASICS

A. Local scale transport description

Transport of a passive solute in the nonsteady, nonuniform flow through a heterogeneous medium can be described at a mesoscopic (local) scale by, e.g., Ref. [5]:

$$\frac{\partial}{\partial t}c(\mathbf{x},t)+\mathbf{u}(\mathbf{x},t)\cdot\boldsymbol{\nabla}c(\mathbf{x},t)-\boldsymbol{\nabla}\mathbf{D}\boldsymbol{\nabla}c(\mathbf{x},t)=\delta(\mathbf{x})\delta(t). \tag{3}$$

The solute concentration is denoted by $c(\mathbf{x},t)$; $\mathbf{u}(\mathbf{x},t)$ and $\mathbf{D}$ are the incompressible local flow velocity and the (constant) dispersion tensor, respectively. The local dispersion tensor in the following is assumed to be diagonal, $D_{ij}=D_{ii}\delta_{ij}$. As boundary conditions we assume a vanishing $c(\mathbf{x},t)$ at the boundaries at infinity. The initial condition for the concentration distribution $c(\mathbf{x},t)$, represented by the right side of Eq. (3), is given by $c(\mathbf{x},t=0)=\delta(\mathbf{x})$. This transport problem will be dealt with in a stochastic modeling framework using a perturbation expansion of $c(\mathbf{x},t)$ in terms of the fluctuations of the random field $\mathbf{u}(\mathbf{x},t)$.

For the following derivations, it is convenient to perform a spatial Fourier transform. The spatial Fourier transform here is defined by:

$$\tilde{c}(\mathbf{k},t)=\int d^dx\,\exp(i\mathbf{k}\cdot\mathbf{x})c(\mathbf{x},t),$$

$$c(\mathbf{x},t)=\int_k \exp(-i\mathbf{k}\cdot\mathbf{x})\tilde{c}(\mathbf{k},t), \tag{4}$$

where we use the shorthand notation $\int_k\cdots\equiv\int d^dk/(2\pi)^d\cdots$. Fourier transformed quantities here and in the following are denoted by a tilde.

B. Stochastic model and ensemble average

We consider the heterogeneous medium as one realization of a spatial random process, the fluctuations of the hydraulic head at the boundaries of the flow domain are modeled as one realization of a temporal random process. The incompressible flow field, which is approximated by the linearized solution of the Darcy equation, see Appendix A, can then be decomposed into

$$u_i(\mathbf{x},t)=u_i(t)-[u_i'(\mathbf{x})+u_i'(\mathbf{x},t)], \tag{5}$$

where the different contributions are defined by, see Ref. [5] and Appendix A,

$$u_i(t)=u[\delta_{i1}-\nu_i(t)], \tag{6}$$

$$u_i'(\mathbf{x})=u\int_k \exp(-i\mathbf{k}\cdot\mathbf{x})p_{i1}(\mathbf{k})\tilde{f}'(\mathbf{k}), \tag{7}$$

$$u_i'(\mathbf{x},t)=-u\int_k \exp(-i\mathbf{k}\cdot\mathbf{x})\nu_l(t)p_{il}(\mathbf{k})\tilde{f}'(\mathbf{k}), \tag{8}$$

where we sum over repeated indices, and the $p_{il}(\mathbf{k})\equiv\delta_{il}-k_ik_l/k^2$. The stationary random field $\boldsymbol{\nu}(t)$ quantifies the normalized time fluctuations of the spatial mean hydraulic (pressure) gradient. The time average is zero by definition $\langle\boldsymbol{\nu}(t)\rangle=0$. The stationary random field $f'(\mathbf{x})$ quantifies the spatial fluctuations of the log-hydraulic conductivity and has zero mean as well, $\overline{f'(\mathbf{x})}=0$. Here and in the following, the ensemble average over all realizations of the temporal random process is denoted by the angular brackets, the average over all realizations of the random medium is denoted by the overbar. Without loss of generality the ensemble mean velocity $\langle\overline{\mathbf{u}(\mathbf{x},t)}\rangle=\mathbf{u}$ is assumed to be aligned with the one-direction of the coordinate system, $u_i=\delta_{i1}u$. The spatial mean velocity is given by Eq. (6), $\overline{\mathbf{u}(\mathbf{x},t)}=\mathbf{u}(t)$, and in general varies in magnitude and direction with time. Owing to the stationarity of the random fields $\boldsymbol{\nu}(t)$ and $f'(\mathbf{x})$, the respective correlation functions read as

$$\langle\nu_l(t)\nu_m(t')\rangle=C_{lm}^{\nu\nu}(t-t'), \tag{9}$$

$$\overline{f'(\mathbf{x})f'(\mathbf{x}')}=C^{ff}(\mathbf{x}-\mathbf{x}'), \tag{10}$$

i.e., depend only on the differences $(t-t')$ and $(\mathbf{x}-\mathbf{x}')$. The correlation functions $C_{lm}^{\nu\nu}(t)$ and $C^{ff}(\mathbf{x})$ here are assumed to be short range, i.e., to decrease sharply for times larger than the correlation time τ and for distances larger than the correlation lengths l_i, $i=1,\ldots,d$, respectively. These definitions allow us to write the velocity autocorrelation functions as:

$$\overline{u_i'(\mathbf{x})u_j'(\mathbf{x}')}=u^2\int_k \exp[-i\mathbf{k}\cdot(\mathbf{x}-\mathbf{x}')]p_{i1}(\mathbf{k})p_{j1}(\mathbf{k})\tilde{C}^{ff}(\mathbf{k}), \tag{11}$$

$$\langle\overline{u_i'(\mathbf{x},t)u_j'(\mathbf{x}',t')}\rangle=u^2\int_k \exp[-i\mathbf{k}\cdot(\mathbf{x}-\mathbf{x}')]\times C_{lm}^{\nu\nu}(t-t')p_{il}(\mathbf{k})p_{jm}(\mathbf{k})\tilde{C}^{ff}(\mathbf{k}), \tag{12}$$

where we sum over identical indices, $i,j=1,\ldots,d$.

For the stochastic analysis of transport in an incompressible turbulent flow field or transport in "frozen" turbulence one usually derives the velocity from a Gauss distributed random vector potential $\mathbf{A}(\mathbf{x},t)$, e.g., Refs. [12,15–17,20,21,23] and does not distinguish between a temporal and a spatial random process,

$$\mathbf{u}(\mathbf{x},t)=\boldsymbol{\nabla}\times\mathbf{A}(\mathbf{x},t). \tag{13}$$

The structure of this flow field is different from the one derived for the flow through a heterogeneous medium in Appendix A. The autocorrelation function of the velocity fluctuations $\mathbf{u}'(\mathbf{x},t)=\mathbf{u}(\mathbf{x},t)-\overline{\mathbf{u}(\mathbf{x},t)}$ for the flow model (13) is given by

$$\overline{u_i'(\mathbf{x},t)u_j'(\mathbf{x}',t')}=\int_k \exp[-i\mathbf{k}\cdot(\mathbf{x}-\mathbf{x}')]\times\left(\delta_{ij}-\frac{k_ik_j}{k^2}\right)\tilde{C}^{uu}(\mathbf{k},t-t') \tag{14}$$

with the autocorrelation spectrum $\tilde{C}^{uu}(\mathbf{k},t-t')$. The overbar here denotes the average over all realizations of the random potential $\mathbf{A}(\mathbf{x},t)$. In this paper, we investigate instead transport in the flow model defined by Eqs. (5) to (12).

C. Observables

As the simplest characteristics for the spatial evolution of the solute, we consider the center of mass velocity and the macroscopic dispersion coefficients of the solute distribution. These are derived from the first and second moments of the concentration distribution,

$$m_i^{(1)}(t)=\int d^dx\,x_ic(\mathbf{x},t)=-i\frac{\partial}{\partial k_i}\tilde{c}(\mathbf{k},t)\Big|_{\mathbf{k}=\mathbf{0}}, \tag{15}$$

$$m_{ij}^{(2)}(t)=\int d^d x x_i x_j c(\mathbf{x},t)=-\frac{\partial^2}{\partial k_i \partial k_j}\tilde{c}(\mathbf{k},t)|_{\mathbf{k}=\mathbf{0}}, \quad (16)$$

where the second equalities in Eqs. (15) and (16), respectively, follow from definition (4) of the Fourier transform. The dispersion coefficients in one realization of the medium are derived from the second centered moments $\kappa_{ij}^{(2)}$ of the concentration distribution, which are defined by

$$\kappa_{ij}^{(2)}(t)=m_{ij}^{(2)}(t)-m_i^{(1)}(t)m_j^{(1)}(t)$$
$$=-\frac{\partial^2}{\partial k_i \partial k_j}\ln\{\tilde{c}(\mathbf{k},t)\}|_{\mathbf{k}=\mathbf{0}}. \quad (17)$$

In the stochastic modeling framework, the observables are defined as averages over all realizations of the spatial and temporal random processes. For transport of a solute in a steady random velocity field, there are two different averaging procedures which lead to the definition of the effective and ensemble dispersion coefficients [32]. We adopt these definitions here for transport in a nonsteady heterogenous flow field. However, note that the order of the averages over the temporal and spatial ensembles gives rise to the definition of four conceptually different dispersion quantities. Recall that the ensemble average over the spatial ensemble is denoted by an overbar, the average over the temporal ensemble is denoted by angular brackets.

We define the effective dispersion coefficient by the time and space ensemble average of the dispersion coefficient (2) in one typical realization of the two random processes:

$$D_{ij}^{\mathrm{eff}}(t)=\frac{1}{2}\frac{d}{dt}\langle\overline{m_{ij}^{(2)}(t)}-\overline{m_i^{(1)}(t)m_j^{(1)}(t)}\rangle$$
$$=-\frac{1}{2}\frac{d}{dt}\frac{\partial^2}{\partial k_i \partial k_j}\langle\overline{\ln\{\tilde{c}(\mathbf{k},t)\}}\rangle|_{\mathbf{k}=\mathbf{0}}. \quad (18)$$

A meaningful ensemble dispersion coefficient is defined by the time average of the spatial ensemble dispersion coefficient in one typical realization of the time random process, i.e., the time average of the dispersion coefficient, which is derived from the space ensemble averaged concentration distribution:

$$D_{ij}^{\mathrm{ens}}(t)=\frac{1}{2}\frac{d}{dt}\langle\overline{m_{ij}^{(2)}(t)}-\overline{m_i^{(1)}(t)}\;\overline{m_j^{(1)}(t)}\rangle$$
$$=-\frac{1}{2}\frac{d}{dt}\frac{\partial^2}{\partial k_i \partial k_j}\langle\ln\{\overline{\tilde{c}(\mathbf{k},t)}\}\rangle|_{\mathbf{k}=\mathbf{0}}. \quad (19)$$

Note that we did not straightforwardly generalize the concepts for steady random flow to transient random flow, as the ensemble dispersion coefficients for steady random flow are derived from the ensemble averaged concentration distribution. From the space and time ensemble averaged concentration distribution one derives the following alternative dispersion quantity:

$$D_{ij}^{(1)}(t)=\frac{1}{2}\frac{d}{dt}\{\langle\overline{m_{ij}^{(2)}(t)}\rangle-\langle\overline{m_i^{(1)}(t)}\rangle\langle\overline{m_j^{(1)}(t)}\rangle\}$$
$$=-\frac{1}{2}\frac{d}{dt}\frac{\partial^2}{\partial k_i \partial k_j}\ln\{\langle\overline{\tilde{c}(\mathbf{k},t)}\rangle\}|_{\mathbf{k}=\mathbf{0}}, \quad (20)$$

which is investigated in Ref. [5]. For completeness we present another average dispersion coefficient, which is defined by the space ensemble average over the dispersion coefficients derived from the time ensemble averaged concentration distribution:

$$D_{ij}^{(2)}(t)=\frac{1}{2}\frac{d}{dt}\{\overline{\langle m_{ij}^{(2)}(t)\rangle}-\overline{\langle m_i^{(1)}(t)\rangle\langle m_j^{(1)}(t)\rangle}\}$$
$$=-\frac{1}{2}\frac{d}{dt}\frac{\partial^2}{\partial k_i \partial k_j}\overline{\ln\{\langle\tilde{c}(\mathbf{k},t)\rangle\}}|_{\mathbf{k}=\mathbf{0}}. \quad (21)$$

In the following we will critically discuss definitions (18)–(21) for the case of transport in the time-dependent flow through a homogeneous medium, i.e., in a time varying spatially constant flow field.

D. Transport in a time-dependent flow field through a homogeneous medium

In order to illustrate and evaluate the different definitions for the ensemble averaged dispersion coefficients (18)–(21) we consider the exactly solvable case of transport of a solute in the time-dependent flow $\mathbf{u}(t)$ through a homogeneous porous medium in the framework of a stochastic model. We consider the fluctuating velocity field $\mathbf{u}(t)$ as one realization of a stationary stochastic process $\{\mathbf{u}(t)\}$, characterized by its mean value $\langle\mathbf{u}(t)\rangle$ and the autocorrelation function $\langle u_i'(t)u_j'(t')\rangle=C_{ij}^{uu}(t-t')$, where we defined $\mathbf{u}(t)\equiv\langle\mathbf{u}(t)\rangle-\mathbf{u}'(t)$. In this case quantities (18) and (19) are equal, and Eqs. (20) and (21), because the respective definitions differ only in the way the spatial average is taken. The transport equation (3) in this case reduces to

$$\frac{\partial}{\partial t}c(\mathbf{x},t)+\mathbf{u}(t)\cdot\nabla c(\mathbf{x},t)-\nabla\mathbf{D}\nabla c(\mathbf{x},t)=\delta(\mathbf{x})\delta(t). \quad (22)$$

The exact solution of Eq. (22) for the concentration of a solute evolving from a pointlike injection at $\mathbf{x}=\mathbf{0}$ in one realization of $\mathbf{u}(t)$ can be easily derived by a spatial Fourier transform of Eq. (22). We obtain

$$c(\mathbf{x},t)=\int_k \exp(-i\mathbf{k}\cdot\mathbf{x})\tilde{c}(\mathbf{k},t)$$
$$=\int_k \exp(-i\mathbf{k}\cdot\mathbf{x})\exp\left(-\mathbf{kDk}t+i\mathbf{k}\cdot\int_0^t dt'\mathbf{u}(t')\right). \quad (23)$$

The center of mass velocity and the dispersion coefficients derived from the concentration distribution (23) are given by $\mathbf{u}(t)$ and the local dispersion coefficients D_{ii}, respectively.

The ensemble and effective dispersion coefficients D_{ij}^{eff} and D_{ij}^{ens}, Eqs. (18) and (19), respectively, are derived from the time average of the dispersion coefficients in one realization of $\mathbf{u}(t)$ and, accordingly, are given by the local dispersion coefficients,

$$D_{ij}^{\mathrm{eff}}(t)=D_{ij}^{\mathrm{ens}}(t)=-\frac{1}{2}\frac{d}{dt}\frac{\partial^2}{\partial k_i \partial k_j}\langle \ln\{\tilde{c}(\mathbf{k},t)\}\rangle|_{\mathbf{k}=\mathbf{0}}$$
$$=\langle D_{ij}\rangle = D_{ij}. \tag{24}$$

The dispersion coefficients defined by Eqs. (20) and (21) in contrast are derived from the ensemble averaged concentration distribution. We assume $\mathbf{u}(t)$ to be a Gaussian random field for simplicity. In this case it is possible to perform the ensemble average of Eq. (23) and give an explicit expression for $\langle c(\mathbf{x},t)\rangle$. Averaging Eq. (23) over the Gaussian random field $\mathbf{u}(t)$, we obtain

$$\langle c(\mathbf{x},t)\rangle = \int_k \exp(-ik_i x_i)\exp\left(-k_i\left\{D_{ij}t+\int_0^t dt'\right.\right.$$
$$\left.\left.\times\int_0^{t'} dt'' C_{ij}^{uu}(t'-t'')\right\}k_j + ik_i\int_0^t dt' \langle u_i(t')\rangle\right), \tag{25}$$

where we sum over identical indices. Thus, for $D_{ij}^{(1)}$ and $D_{ij}^{(2)}$ we obtain

$$D_{ij}^{(1)}(t)=D_{ij}^{(2)}(t)=-\frac{1}{2}\frac{d}{dt}\frac{\partial^2}{\partial k_i \partial k_j}\ln\{\langle \tilde{c}(\mathbf{k},t)\rangle\}|_{\mathbf{k}=\mathbf{0}}$$
$$=D_{ij}+\int_0^t dt' C_{ij}^{uu}(t'). \tag{26}$$

Using Eqs. (6) and (9) for the temporally fluctuating flow field (in this case $C_{ij}^{uu}\equiv u^2 C_{ij}^{\nu\nu}$), we obtain for Eq. (26) in the limit $t\to\infty$,

$$\lim_{t\to\infty} D_{ij}^{(1)}(t)=D_{ij}+u^2\sigma_{ij}^2\tau_{ij}, \tag{27}$$

where σ_{ij}^2 is the variance of the time fluctuations of $\mathbf{u}(t)$ and τ_{ij} is the correlation time $[\tau_{ij}\equiv\int_0^\infty dt C_{ij}^{\nu\nu}(t)/\sigma_{ij}^2]$. Expression (27) is identical to the result derived in Ref. [5] for the macrodispersivity in a time-fluctuating flow field and was identified as the leading disorder contribution due to a temporally fluctuating flow field. However, as we see by comparison to the dispersion coefficients in one single realization of the random flow field $\mathbf{u}(t)$, this contribution does not characterize the true effective spreading of the solute plume in one realization of the medium. Thus, the dispersion coefficients defined by Eqs. (21) and (20) are not self-averaging observables. They do not represent dynamic quantities which characterize the effective large scale transport behavior but rather serve as an uncertainty estimate for the concentration in time-fluctuating flow fields. Thus, also the time ensemble averaged concentration distribution (25), which has been considered in Ref. [10] is not representative for the concentration distribution in a typical realization of the random process. In the following, we will focus on the analysis of D_{ij}^{eff} and D_{ij}^{ens} defined by Eqs. (18) and (19), respectively.

E. Integral equation and perturbation series

Now we will derive an integral equation for the concentration distribution $c(\mathbf{x},t)$ using decomposition (5) of the random velocity field into the constant mean value and fluctuations about it. The transport equation (3) can be rewritten as

$$\frac{\partial}{\partial t}c(\mathbf{x},t)+\mathbf{u}(t)\cdot\nabla c(\mathbf{x},t)-\nabla\mathbf{D}\nabla c(\mathbf{x},t)$$
$$=[\mathbf{u}'(\mathbf{x})+\mathbf{u}'(\mathbf{x},t)]\cdot\nabla c(\mathbf{x},t). \tag{28}$$

For technical convenience we perform a spatial Fourier transform (4). Equation (28) reads in Fourier space

$$\frac{\partial}{\partial t}\tilde{c}(\mathbf{k},t)-\{i\mathbf{k}\cdot\mathbf{u}(t)-\mathbf{kDk}\}\tilde{c}(\mathbf{k},t)$$
$$=-\int_{k'} i\mathbf{k}\cdot[\tilde{\mathbf{u}}'(\mathbf{k}')+\tilde{\mathbf{u}}'(\mathbf{k}',t)]\tilde{c}(\mathbf{k}-\mathbf{k}',t). \tag{29}$$

The transport equation (29) can be transformed into an equivalent integral equation:

$$\tilde{c}(\mathbf{k},t)=\tilde{c}_0(\mathbf{k},t)-\int_{k'}\int_0^t dt'\tilde{c}_0(\mathbf{k},t-t')i\mathbf{k}\cdot[\tilde{\mathbf{u}}'(\mathbf{k}')$$
$$+\tilde{\mathbf{u}}'(\mathbf{k}',t')]\tilde{c}(\mathbf{k}-\mathbf{k}',t'). \tag{30}$$

The propagator $\tilde{c}_0(\mathbf{k},t)$ is given by

$$\tilde{c}_0(\mathbf{k},t)=\exp\left\{-\mathbf{kDk}t+i\mathbf{k}\cdot\int_0^t dt'\mathbf{u}(t')\right\}, \tag{31}$$

i.e., we expand about the solution of Eq. (28) for $\mathbf{u}'(\mathbf{x})\equiv 0$. Equation (30) is the starting point for the perturbative solution of the transport problem.

By iteration of the integral equation (30), we obtain the perturbation series:

$$\tilde{c}(\mathbf{k},t)=\tilde{c}_0(\mathbf{k},t)-\int_{k'}\int_0^t dt'\tilde{c}_0(\mathbf{k},t-t')i\mathbf{k}\cdot[\tilde{\mathbf{u}}'(\mathbf{k}')$$
$$+\tilde{\mathbf{u}}'(\mathbf{k}',t')]\tilde{c}_0(\mathbf{k}-\mathbf{k}',t')$$
$$+\int_{k'}\int_{k''}\int_0^t dt'\int_0^{t'} dt''\tilde{c}_0(\mathbf{k},t-t')i\mathbf{k}\cdot[\tilde{\mathbf{u}}'(\mathbf{k}')$$
$$+\tilde{\mathbf{u}}'(\mathbf{k}',t')]\tilde{c}_0(\mathbf{k}-\mathbf{k}',t'-t'')i(\mathbf{k}-\mathbf{k}')\cdot[\tilde{\mathbf{u}}'(\mathbf{k}'')$$
$$+\tilde{\mathbf{u}}'(\mathbf{k}'',t'')]\tilde{c}_0(\mathbf{k}-\mathbf{k}'-\mathbf{k}'',t'')+\cdots. \tag{32}$$

This perturbation series for $\tilde{c}(\mathbf{k},t)$, truncated after the second order in $\tilde{\mathbf{u}}'$, is the basis for the following perturbative analysis.

In the following we focus on the contributions to the ensemble and effective dispersion coefficients due to temporal and spatial fluctuations of the velocity field. The ensemble averaged center of mass velocity is given by the ensemble mean flow velocity u,

$$u_i^{\mathrm{cm}}(t)=\frac{d}{dt}\langle\overline{m_i^{(1)}(t)}\rangle=u\,\delta_{i1}. \tag{33}$$

This can be easily seen by inserting Eq. (32) into Eq. (15) and averaging the resulting expression. The effective and ensemble dispersion coefficients are obtained by substituting Eq. (32) into Eqs. (18) and (19), respectively. Expanding the resulting expression consistently up to second order in $\mathbf{u}'$ leads to

$$D_{ij}^{\mathrm{eff}}(t)=D_{ii}+\delta^{(s)}\{D_{ij}^{\mathrm{eff}}\}(t)+\delta^{(t)}\{D_{ij}^{\mathrm{eff}}\}(t), \tag{34}$$

$$D_{ij}^{\mathrm{ens}}(t)=D_{ii}+\delta^{(s)}\{D_{ij}^{\mathrm{ens}}\}(t)+\delta^{(t)}\{D_{ij}^{\mathrm{ens}}\}(t), \tag{35}$$

where $\delta^{(s)}\{D_{ij}^{\mathrm{eff}}\}(t)$ and $\delta^{(s)}\{D_{ij}^{\mathrm{ens}}\}(t)$ denote the second-order contributions to the effective and ensemble dispersion coefficients, respectively, due to a time-independent heterogeneous flow field. They are well known. The asymptotic limit of $\delta^{(s)}\{D_{ii}^{\mathrm{ens}}\}(t)$ has been determined in Ref. [2]. The time evolution of both quantities has been determined in Refs. [36,38,39] for $d=2$ and $d=3$ spatial dimensions. The contributions due to temporal and spatial fluctuations are given by

$$\delta^{(t)}\{D_{ij}^{\mathrm{ens}}\}(t)=\int_k\int_0^t dt'\tilde{g}_0(\mathbf{k},t')C_{lm}^{\nu\nu}(t')p_{il}(\mathbf{k})p_{jm}(\mathbf{k})\tilde{C}^{ff}(\mathbf{k}), \tag{36}$$

$$\delta^{(t)}\{D_{ij}^{\mathrm{eff}}\}(t)=\delta^{(t)}\{D_{ij}^{\mathrm{ens}}\}(t)-\int_k\int_0^t dt'\tilde{g}_0(-\mathbf{k},t)\tilde{g}_0(\mathbf{k},t')\times C_{lm}^{\nu\nu}(t-t')p_{il}(\mathbf{k})p_{jm}(\mathbf{k})\tilde{C}^{ff}(\mathbf{k}), \tag{37}$$

where the propagator $\tilde{g}_0(\mathbf{k},t)$ is defined by the ensemble mean velocity equivalent of Eq. (31),

$$\tilde{g}_0(\mathbf{k},t)\equiv\exp(-\mathbf{kDk}t+iuk_1t). \tag{38}$$

We disregard contributions to Eq. (31) of order ν for consistency.

The effective and ensemble dispersion coefficients (18) and (19) do not have contributions due to temporal fluctuations only. Apparently the contributions to the effective transport behavior of a solute result from the interplay of spatial and temporal fluctuations as a consequence of the assumption of constant local dispersion (Refs. [7,8]).

Using Eq. (38) for $\tilde{g}_0(\mathbf{k},t)$ in Eqs. (36) and (37), we obtain

$$\delta^{(t)}\{D_{ij}^{\mathrm{ens}}\}(t)=ul_1M_{ij}^{+}(t,\mathbf{A})|_{(A_l=1,l=1,\dots,d)}, \tag{39}$$

$$\delta^{(t)}\{D_{ij}^{\mathrm{eff}}\}(t)=ul_1[M_{ij}^{+}(t,\mathbf{A})|_{(A_l=1,l=1,\dots,d)}-M_{ij}^{-}(t,\mathbf{A})|_{(A_l=1+4t/\tau_{D_l},l=1,\dots,d)}]. \tag{40}$$

The auxiliary functions $M_{ij}(t,\mathbf{A})$ are defined by

$$M_{ij}^{\pm}(t,\mathbf{A})=(2\pi)^{d/2}\int_k\int_0^{t/\tau_u}dt'\exp\left(-\frac{k_l^2}{2}(A_l\pm2\epsilon_lt'-1)+ik_1t'\right)C_{lm}^{\nu\nu}(t'\tau_u)\tilde{C}_{ff}^{*}(\mathbf{k})p_{il}^{*}(\mathbf{k})p_{jm}^{*}(\mathbf{k}), \tag{41}$$

where we sum over repeated indices. We defined here the vector $\mathbf{A}$ in order to unify the notation. When $M^{\pm}$ is used in the expression for $\delta^{(t)}\{D_{ij}^{\mathrm{ens}}\}$, the coefficients of $\mathbf{A}$ are given by $A_l=1$. When used in the expression for $\delta^{(t)}\{D_{ij}^{\mathrm{eff}}\}$, they are given by $A_l=1+4t/\tau_{D_l}$. For compactness we defined $\tilde{C}_{ff}^{*}(\mathbf{k})\equiv\tilde{C}_{ff}(k_1/l_1,\dots,k_d/l_d)$ and $p_{ij}^{*}(\mathbf{k})\equiv p_{ij}(k_1/l_1,\dots,k_d/l_d)$. We defined the advection time scale $\tau_u\equiv l_1/u$ which measures the time for the advective transport of the solute over one correlation length of the medium. Furthermore, we defined the dispersion time scales $\tau_{D_l}\equiv l_l^2/D_{ll}$, $l=1,\dots,d$, which characterize the time for dispersive solute transport over the respective correlation length [36]. The $\epsilon_l\equiv\tau_u/\tau_{D_l}=D_{ll}l_1/(ul_l^2)$, $l=1,\dots,d$, denote the inverse Peclet numbers which for realistic aquifer situations are much smaller than 1, $\epsilon_l\ll1$ [2]. The nondimensional Kubo number $\kappa\equiv u\tau/l_1$ [23] characterizes transport in time-dependent heterogeneous flow fields. It compares the distance $l_\kappa\equiv u\tau$ ("Kubo distance") the solute is advected by the mean flow during the correlation time τ to the correlation length in mean flow direction l_1, $\kappa=l_\kappa/l_1$; it equivalently compares the correlation time τ to the advection time scale τ_u, $\kappa=\tau/\tau_u$.

III. CONTRIBUTIONS TO THE DISPERSION COEFFICIENTS

For simplicity, in the following we investigate a scenario in which the direction of the spatial mean velocity $\mathbf{u}(t)$, Eq. (6), does not vary in time, i.e.,

$$\nu_i(t)\equiv\delta_{i1}\nu(t). \tag{42}$$

Note, however, that, as implied by Eq. (8), time fluctuations of the spatial mean velocity in the one direction drive temporal fluctuations of the transverse velocity components. The time behavior of the contributions due to random variations of the direction of $\mathbf{u}(t)$ is similar to the time behavior that will be presented in the following for assumption (42).

Using Eq. (42), the correlation matrix (9) reduces to $C_{lm}^{\nu\nu}(t)\equiv\delta_{l1}\delta_{m1}C^{\nu\nu}(t)$. Inserting this expression into Eqs. (36) and (37), we obtain the following simplified expressions for the contributions to the effective and ensemble dispersion coefficients:

$$\delta^{(t)}\{D_{ii}^{\mathrm{ens}}\}(t)=\int_0^t dt'\,C^{\nu\nu}(t')\frac{d}{dt'}\,\delta^{(s)}\{D_{ii}^{\mathrm{ens}}\}(t'), \quad (43)$$

$$\delta^{(t)}\{D_{ii}^{\mathrm{eff}}\}(t)=\delta^{(t)}\{D_{ii}^{\mathrm{ens}}\}(t)-\int_k\int_0^t dt'\,\tilde{g}_0(-\mathbf{k},t)\tilde{g}_0(\mathbf{k},t')\times p_{i1}(\mathbf{k})^2\tilde{C}^{ff}(\mathbf{k})C^{\nu\nu}(t-t'), \quad (44)$$

where the nondiagonal coefficients vanish because of symmetry. Time fluctuations of the direction of $\mathbf{u}(t)$ may induce nonvanishing contributions to the off-diagonal dispersion coefficients.

The correlation function $C^{\nu\nu}(t)$ decays sharply for times large compared to the correlation time scale τ and thus has the effect of a cutoff for the time integrations in expressions (43) and (44). In the following we employ a Gaussian shaped time correlation function,

$$C^{\nu\nu}(t)=\sigma_{\nu\nu}^2\exp\left(-\frac{t^2}{2\tau^2}\right), \quad (45)$$

where $\sigma_{\nu\nu}^2$ denotes the variance of time fluctuations.

Furthermore, we also assume a Gaussian shaped correlation function for the fluctuations of the log-hydraulic conductivity,

$$C^{ff}(\mathbf{x})=\sigma_{ff}^2\prod_{i=1}^d \exp[-x_i^2/(2l_i^2)], \quad (46)$$

where σ_{ff}^2 denotes the variance of the spatial fluctuations; the l_i are the correlation lengths in i direction. The autocorrelation spectrum $\tilde{C}^{ff}(\mathbf{k})$ of the log-hydraulic conductivity $f(\mathbf{x})$ then is given by

$$\tilde{C}^{ff}(\mathbf{k})=\sigma_{ff}^2\prod_{i=1}^d (2\pi l_i^2)^{1/2}\exp(-k_i^2l_i^2/2). \quad (47)$$

In the following, we will focus on isotropic disorder scenarios, i.e., $l_1=\cdots=l_d$.

Using Eq. (42) and inserting Eqs. (45) and (47) into Eq. (41), we obtain for the auxiliary functions $M_{ii}^{\pm}(t,\mathbf{A})$:

$$M_{ii}^{\pm}(t,\mathbf{A})=(2\pi)^{d/2}\sigma_{\nu\nu}^2\sigma_{ff}^2\int_k\int_0^{t/\tau_u}dt'\exp\left(-\frac{k_l^2}{2}(A_l\pm2\epsilon_l t')+ik_1t'\right)\exp\left(-\frac{t'^2}{2(\tau/\tau_u)^2}\right)p_{i1}^*(\mathbf{k})^2, \quad (48)$$

where we sum over repeated indices (l).

In Appendix B 2 we give integral expressions for the $M_{ii}(t,\mathbf{A})$ for $d=3$ and $d=2$ spatial dimensions, which are evaluated numerically in order to investigate the complete time behavior of the lowest-order contribution due to a temporally and spatially fluctuating flow field. Furthermore, we give approximate analytical expressions in Appendix B 2 a for Eq. (48) applying the approximation for $\epsilon_l \ll 1$ and $t \gg \tau_u$ presented in Ref. [36]. Explicit expressions for Eq. (48) in $d=2$ dimensions for the limiting case of $D_{11}=D_{22}=0$ are given in Appendix B 2 b.

In the following all results for the dispersion coefficients are normalized by $\sigma_{ff}^2\sigma_{\nu\nu}^2ul_1$.

A. Asymptotic behavior

It is well documented in the literature, e.g., Ref. [2], that the contributions to the asymptotic transverse dispersion coefficients due to a steady spatially varying flow field are of the order of magnitude of the local dispersion coefficients in lowest-order perturbation theory. This is in contradiction to experimental results. Numerical simulations [38] have shown that in $d=3$ spatial dimensions there are macroscopic contributions resulting from higher-order terms of the perturbation series (32). In $d=2$ spatial dimensions, however, there are no macroscopic contributions to the asymptotic transverse dispersion coefficients, which has been shown numerically [39] as well as analytically without invoking perturbation theory for the general case of an incompressible steady random field [40]. For a temporally fluctuating flow field the situation is different.

We consider the asymptotic behavior of the contributions to the dispersion coefficients for isotropic local dispersion, $D_{11}=\cdots=D_{dd}\equiv D$ as a function of the Kubo number κ. As for a steady velocity field [36], in the limit $t\to\infty$ the contributions to the ensemble and effective dispersion coefficients converge to the same asymptotic value:

$$\lim_{t\to\infty}\delta^{(t)}\{D_{ii}^{\mathrm{eff}}\}(t)=\lim_{t\to\infty}\delta^{(t)}\{D_{ii}^{\mathrm{ens}}\}(t)\equiv\delta^{(t)}\{D_{ii}^{\infty}\}(\kappa). \quad (49)$$

Because the contributions to the transverse dispersion coefficients are equal for the considered scenario we define for the following $\delta^{(t)}\{D_L^{\infty}\}(\kappa)\equiv\delta^{(t)}\{D_{11}^{\infty}\}(\kappa)$ and $\delta^{(t)}\{D_T^{\infty}\}(\kappa)\equiv\delta^{(t)}\{D_{ii}^{\infty}\}(\kappa)$, $i\neq1$.

Figures 1(a) and 1(b) illustrate the behavior of $\delta^{(t)}\{D_L^{\infty}\}(\kappa)$ and $\delta^{(t)}\{D_T^{\infty}\}(\kappa)$ in $d=3$ and $d=2$ dimensions, respectively, for f $\epsilon=10^{-3}$ and $\epsilon=0$. Analytical expressions for $\delta^{(t)}\{D_L^{\infty}\}(\kappa)$ and $\delta^{(t)}\{D_T^{\infty}\}(\kappa)$ for $\epsilon=0$ are given in Appendix B 1.

In the limit $\kappa\to0$, $\delta^{(t)}\{D_L^{\infty}\}(\kappa)$ and $\delta^{(t)}\{D_T^{\infty}\}(\kappa)$ tend to zero because the fluctuations of the velocity field are too fast to contribute remarkably to the mixing of the solute. From there, the contributions to the dispersion coefficients increase linearly with κ for $\kappa\lesssim1$,

$$\delta^{(t)}\{D_i^{\infty}\}(\kappa)=a_i\sigma_{ff}^2\sigma_{\nu\nu}^2lu\kappa+\cdots, \quad (50)$$

$i=L,T$, where the slope $a_L=4\sqrt{2\pi}/15$, $a_T=\sqrt{2\pi}/30$ in $d=3$, and $a_L=3\sqrt{2\pi}/16$, $a_T=\sqrt{2\pi}/16$ in $d=2$, respectively. The dots in Eq. (50) denote subleading contributions. The longitudinal coefficient tends to its maximum of about $\sqrt{\pi/2}\sigma_{ff}^2\sigma_{\nu\nu}^2lu$ asymptotically $\sim\kappa^{-(d-1)}$ in the limit $\kappa\to\infty$, but is close to this limit already for $\kappa\approx10$. The transverse coefficient reaches its maximum for $\kappa\approx1$ and is $\approx0.05\sigma_{ff}^2\sigma_{\nu\nu}^2lu$ in $d=3$ and $\approx0.12\sigma_{ff}^2\sigma_{\nu\nu}^2lu$ in $d=2$. From

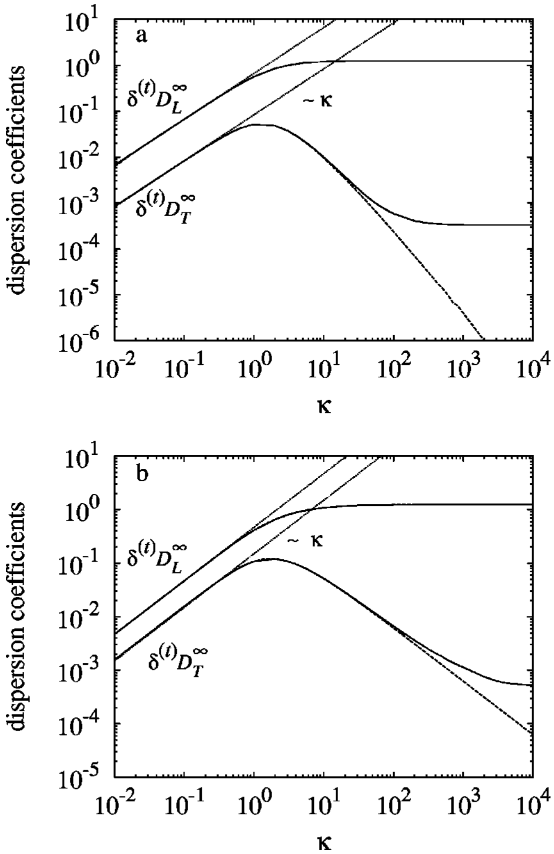

FIG. 1. Behavior of the second-order contributions to the longitudinal and transverse asymptotic dispersion coefficients (scaled by $ul\sigma_{ff}^2\sigma_{\nu\nu}^2$) as a function of the Kubo number κ $(=\tau/\tau_u)$ in (a) $d=3$ and (b) $d=2$ for an inverse Peclet number $\epsilon=10^{-3}$. Note that, when $\tau<\tau_u$, i.e., $u\tau<l$, $\delta^{(t)}\{D_T^\infty\}=1/8\delta^{(t)}\{D_L^\infty\}$ for $d=3$ and $\delta^{(t)}\{D_T^\infty\}=1/3\delta^{(t)}\{D_L^\infty\}$ for $d=2$. The dashed lines in (a) and (b) describe the behavior of $\delta^{(t)}\{D_L^\infty\}$ and $\delta^{(t)}\{D_T^\infty\}$ for $\epsilon=0$ according to Eqs. (B1)–(B4), respectively. For the longitudinal coefficients the curves for $\epsilon=0$ and $\epsilon=10^{-3}$ are practically indistinguishable. The dotted lines are the respective approximations (50) for small κ.

there, $\delta^{(t)}\{D_T^\infty\}$ tends to a value of the order of the (microscopic) local dispersion coefficient $\sim\kappa^{-(d-1)}$ for $\kappa\to\infty$. Note that here the order of the limits is important, we first take the limit $t\to\infty$ and then we look at the behavior for $\kappa\to\infty$. In the hypothetical case $\kappa\to\infty$ and finite times, the ensemble averaged quantities have only a restricted formal meaning because for $t/\tau_u<\kappa$ the flow field is quasisteady but the fluctuations from realization to realization are large.

Note that the contributions to the longitudinal as well as to the transverse dispersion coefficients are of macroscopic order of magnitude, in $d=3$ and $d=2$. It is worth noticing the sizable contribution of the temporal fluctuations to the transverse dispersion coefficients, despite the fact that the spatial mean velocity $\mathbf{u}(t)$ does not fluctuate laterally. For $\kappa\lesssim1$, i.e., $\tau\lesssim\tau_u$, which is important for field applications [5], the transverse coefficients have values of about $\delta^{(t)}\{D_L^\infty\}/8$ and $\delta^{(t)}\{D_L^\infty\}/3$ for $d=3$ and $d=2$, respectively. It is worth pointing out that the empirical ratio between the transverse and longitudinal dispersion usually adopted by hydrogeologists falls in this range [41].

B. Time behavior

In the following, we consider the contributions to the effective and ensemble dispersion coefficients due to the interaction of spatial and temporal fluctuations of the random flow field for different scenarios. At first we investigate an isotropic scenario with isotropic local dispersion in order to systematically study the differences between the effective and ensemble dispersion coefficients for different Kubo numbers in $d=2$ and $d=3$ dimensions. Then we study the behavior for various anisotropic local dispersion scenarios in $d=2$ and $d=3$ dimensions. Note that for $t/\tau_u<\max(\kappa,1)$, the dispersion coefficients, which are determined as ensemble averages, have only a limited formal meaning. For $t/\tau_u<\kappa$, the flow field is quasisteady while the sample to sample fluctuations of the temporal stochastic process, of course, are large. For $t/\tau_u<1$, the solute plume has not yet been advectively transported over one correlation length of the medium and thus the medium looks homogeneous. But of course there are large fluctuations from realization to realization of the spatial random process, which models the medium heterogeneities [36].

1. Isotropic local dispersion

We consider here a scenario with isotropic local dispersion, i.e., $D_{11}=\cdots=D_{dd}=D$. The different inverse Peclet numbers ϵ_i and dispersion time scales τ_{D_i} reduce to $\epsilon_1=\cdots=\epsilon_d=D/(ul)$ and $\tau_{D_1}=\cdots=\tau_{D_d}=l^2/D$, respectively. Furthermore, for this scenario the contributions to the transverse dispersion coefficients in d dimensions are equal and we define $\delta^{(t)}\{D_{11}^{\text{eff}}\}(t)\equiv\delta^{(t)}\{D_L^{\text{eff}}\}(t)$ and $\delta^{(t)}\{D_{ii}^{\text{eff}}\}(t)\equiv\delta^{(t)}\{D_T^{\text{eff}}\}(t)$, $i\neq1$, and for the ensemble dispersion coefficients accordingly.

Figures 2 and 3 illustrate the time evolution of the contributions to the longitudinal and transverse effective and ensemble dispersion coefficients for $d=3$ and $d=2$, respectively, and the corresponding approximations for $\epsilon\ll1$ and $t\gg\tau_u$, Appendix B 2 a. The dispersion time scale is $\tau_D=10^3\tau_u$, the inverse Peclet number is given by $\epsilon=10^{-3}$. The advection and dispersion time scales τ_u and τ_D are clearly separated. The quality of the approximate expressions is very good for $t/\tau>\kappa$, where the stochastic approach is assumed to be valid. For large Kubo numbers, the transverse effective and ensemble coefficients, Figs. 3(a) and 3(b), are only poorly described by the approximate expressions, because the approximations disregard contributions of order ϵ. For large κ, however, the long-time values themselves are of the order of ϵ and so terms of this order of magnitude become important.

The contributions to the longitudinal dispersion coefficients are shown in Figs. 2(a) and 2(b). As for steady random flow [36], one observes a qualitatively and quantitatively different time behavior for $\delta^{(t)}\{D_L^{\text{eff}}\}$ and $\delta^{(t)}\{D_L^{\text{ens}}\}$ for finite times.

In the long-time limit, the effective observables converge to the ensemble values and assume their (constant) asymptotic long-time values, which depend on the Kubo number as discussed in the preceding section. The interaction

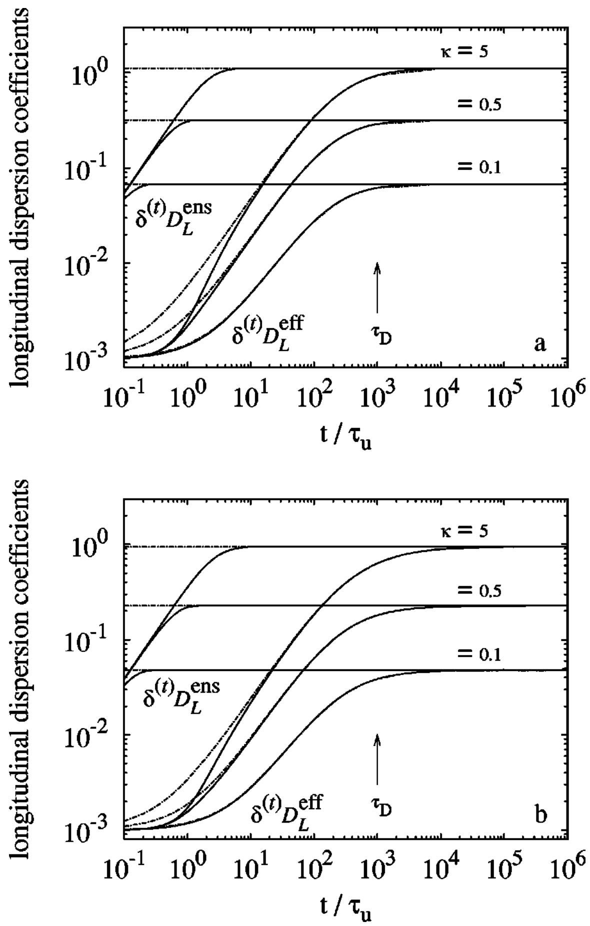

FIG. 2. Time behavior of the contributions to the longitudinal ensemble and effective dispersion coefficients in (a) $d=3$ and (b) $d=2$ spatial dimensions for $\epsilon=10^{-3}$, $\kappa=0.1$, $\kappa=0.5$, and $\kappa=5$. The dash-dotted lines are the corresponding approximations for small ϵ and $t \gg \tau_u$.

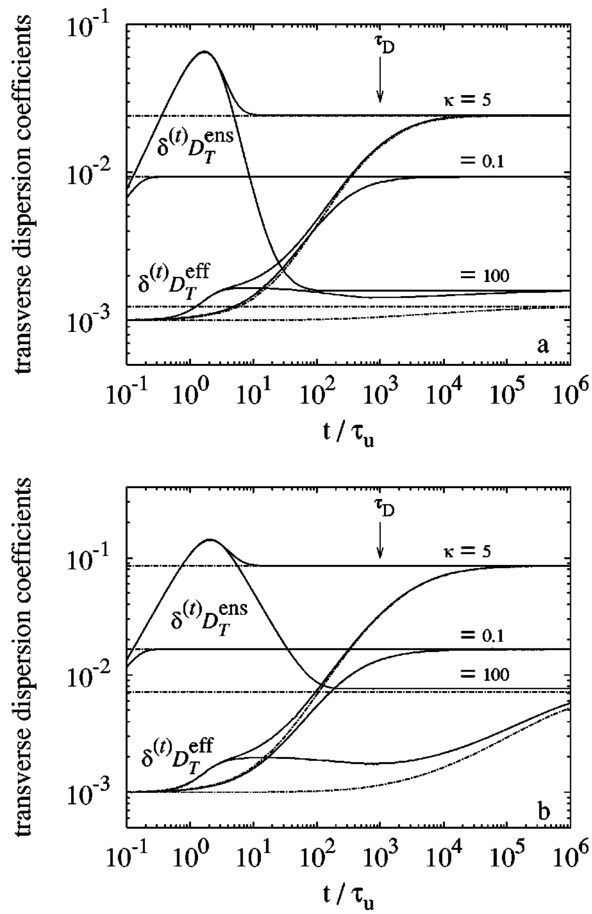

FIG. 3. Time behavior of the contributions to the transverse ensemble and effective dispersion coefficients in $d=3$ and $d=2$ spatial dimensions for $\tau_D=10^3\tau_u$, $\epsilon=10^{-3}$, $\kappa=0.1$, $\kappa=5$, and $\kappa=100$. The dash-dotted lines are the corresponding approximations for small ϵ and $t \gg \tau_u$.

of the time fluctuations and the sample to sample fluctuations of the center of mass leads to a fast increase of $\delta^{(t)}\{D_L^{\text{ens}}\}$ to its long-time value on the correlation time scale. The fluctuations of the center of mass are an artificial, purely advective, and nonphysical ensemble dispersion effect [36], which is visible also in the hypothetical situation of zero local dispersion, see the explicit expression for $D=0$ given in Appendix B 2 b. For zero local dispersion, the effective dispersion coefficients are zero by definition, because the dispersion coefficients in one realization are zero. However, in the presence of local dispersion as a transverse mixing mechanisms both quantities converge, Figs. 2 and 3, and the macroscale dispersion due to advective fluctuations becomes a real effect. The local scale transverse mixing here is enhanced by the time fluctuations of the velocity field, which leads to a behavior that is quantitatively different from the one observed for steady random flow fields.

The contribution to the longitudinal ensemble dispersion coefficient approaches its asymptotic long-time value exponentially on the correlation time scale τ, see Appendix B 2 b. In a steady random field, the ensemble coefficient evolves algebraically on the advective time scale [36]. The influence of the temporal variations of the flow field on the behavior of the effective coefficients is more subtle. The time fluctuations affect the evolution of the effective quantity by both the interplay with the spatial heterogeneities and local dispersion. In Figs. 2(a) and 2(b) we observe that for $t \gg \tau_D$ the effective coefficients evolve slightly slower to their asymptotic values as κ increases. In fact, from the approximate expressions given in Appendix B 2, we identify a new time scale $\tau_\kappa \equiv \tau_D \kappa^2 = l_\kappa^2/D$, which measures the time for the local dispersive spreading of the solute over the typical distance $l_\kappa = u\tau$ ("Kubo distance") the solute is advected during one correlation time τ. If the Kubo number $\kappa \gg 1$, i.e., $l_\kappa \gg l_1$, the effective coefficient evolves approximately as $t^{-(d-1)/2}$ for $\tau_D \ll t \ll \tau_\kappa$, which is identical to the behavior observed in steady random flow [36]. Apparently, the transport times in $\tau_D \ll t \ll \tau_\kappa$ are so small that the temporal fluctuations, which are characterized by the Kubo length $l_\kappa \gg l_1$, have no effect yet on the local spreading of the solute and the transport behavior is similar to the one observed for a steady flow field.

For the long-time regime $t \gg \tau_\kappa$ (for $\kappa \gg 1$) the approximate expressions given in Appendix B 2 for the effective longitudinal dispersion coefficient lead to

$$\delta^{(t)}\{D_L^{\infty}\} - \delta^{(t)}\{D_L^{\text{eff}}\} \sim t^{-d/2}. \tag{51}$$

For κ of the order of or smaller than 1, the asymptotic long-time regime is reached according to $t^{-d/2}$ already for $t \gg \tau_D$. Thus, the relevant time regimes and the exponents by which the effective quantity evolves asymptotically depend on the Kubo number κ. This explains the slightly different asymptotic behavior observed in Figs. 2(a) and 2(b) for different κ.

Figures 3(a) and 3(b) display the behavior of the contributions to the transverse dispersion coefficients in $d=3$ and $d=2$, respectively. The behavior of the effective and ensemble coefficients is qualitatively and quantitatively different from the one observed in steady random flows [36]. The effective and ensemble quantities evolve to a macroscopic asymptotic value that depends on the Kubo number κ as discussed in the preceding section. As observed for the longitudinal ensemble coefficient, the transverse ensemble coefficients approach their asymptotic (macroscopic) long-time values exponentially on the correlation scale τ, see Appendix B 2 b.

For $\kappa \gg 1$, the effective coefficients approach their (macroscopic) asymptotic long-time values for $t \gg \tau_\kappa$ as

$$\delta^{(t)}\{D_T^{\infty}\} - \delta^{(t)}\{D_T^{\text{eff}}\} \sim t^{-d/2}. \tag{52}$$

For κ of the order of or smaller than 1, the long-time value is reached according to Eq. (52) already for $t \gg \tau_D$, which explains that the effective coefficients in Figs. 3(a) and 3(b) evolve earlier to their asymptotic value for decreasing κ. Note that the longitudinal and effective coefficients show the same asymptotic long-time behavior, which indicates that the same local spreading mechanisms activate the macroscopic advective spreading. For steady random flow the spatial contrasts of the transverse velocity components are not sufficient to lead to macroscopic transverse dispersion coefficients. Temporal fluctuations, however, amplify these contrasts and as a consequence macroscopic transverse spreading is activated by local dispersion mechanisms.

2. Anisotropic local dispersion and isotropic disorder correlation

In this section, we study the time behavior of the disorder-induced contributions to the effective and ensemble dispersion coefficients for anisotropic local dispersion. The inverse Peclet numbers are given by $\epsilon_i = D_{ii}/(ul)$, and the dispersion time scales by $\tau_{D_i} = l^2/D_{ii}$ for $i=1,\ldots,d$.

In a steady random field, the evolution of the longitudinal effective dispersion coefficient is determined by the transverse local dispersion time scales, τ_{D_i}, $i \neq 1$ [36]. The transverse spreading by local dispersion makes the solute sample the heterogeneities in one medium and activates the "advective" spreading due to the complicated streamline structure, which then leads to macrodispersion. These mechanisms can be observed for transport in a time-dependent velocity field as well.

a. Vanishing longitudinal local dispersion coefficient. Figures 4(a) and 4(b) illustrate the contributions to the longitudinal and transverse dispersion coefficients, respectively, for vanishing longitudinal local dispersion, $\epsilon_1 = 0$ and $\epsilon_2 = 10^{-2}$ in $d=2$. The behavior in $d=3$ is qualitatively the same and not displayed here.

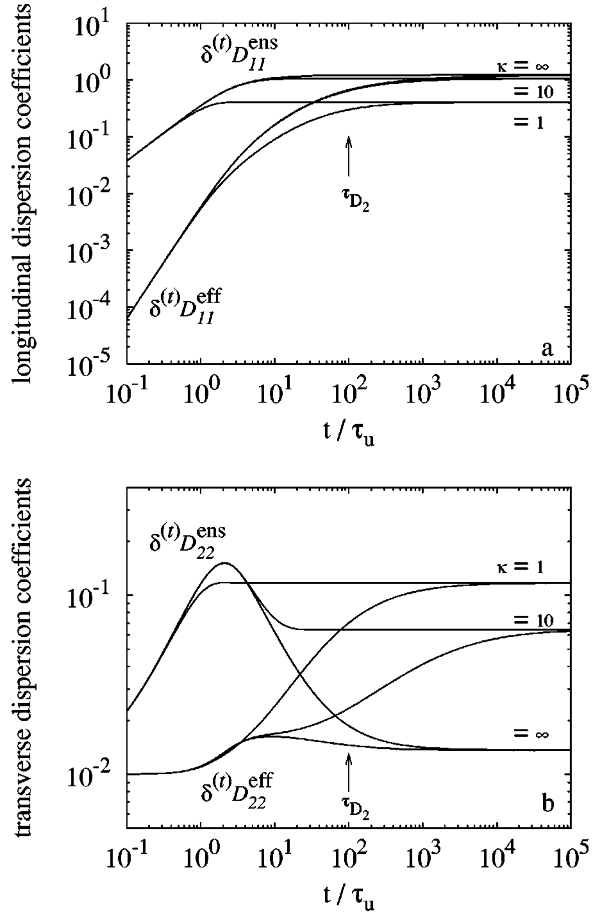

FIG. 4. Time behavior of the contributions to the (a) longitudinal and (b) transverse ensemble and effective dispersion coefficients in $d=2$ dimensions, $\kappa = 1,10,\infty$, $\epsilon_1 = 0$, $\epsilon_2 = 10^{-2}$.

For large times, the effective longitudinal coefficients evolve to their asymptotic long-time value and the behavior is similar to the one observed for isotropic local dispersion in the preceding section. As observed there, the long-time behavior depends on the value of the Kubo number κ. For large κ, the behavior of the longitudinal effective coefficient in the intermediate regime $\tau_{D_2} \ll t \ll \tau_{\kappa_2}$, with $\tau_{\kappa_2} = \tau_{D_2}\kappa^2$, is given by

$$\delta^{(t)}\{D_L^{\infty}\} - \delta^{(t)}\{D_L^{\text{eff}}\} \sim t^{-(d-1)/2}, \tag{53}$$

which is the same as for transport in a steady flow field [36] and observed for isotropic local dispersion in the preceding section. In the long-time regime $t \gg \tau_{\kappa_2}$ (for $\kappa \gg 1$) the effective longitudinal coefficient then evolves algebraically $\sim t^{-d/2}$ as in the isotropic case. For κ of the order of or smaller than 1 the longitudinal coefficients approach their asymptotic long-time values already for $t \gg \tau_D$. Thus, for $\kappa = 1$ the effective coefficient reaches its asymptotic long-time value faster than for $\kappa = 10$ as illustrated in Fig. 4(a).

A similar time behavior is observed for the transverse effective coefficients, Fig. 4(b). For $\kappa=1$, the evolution is faster than for $\kappa=10$. In the asymptotic long-time regimes $t \gg \tau_{\kappa_2}$ (for $\kappa \gg 1$) and $t \gg \tau_D$ (for κ of the order of or smaller than 1), respectively, the effective coefficient evolves like the longitudinal coefficient $\sim t^{-d/2}$.

b. Vanishing transverse local dispersion coefficients. Now we consider a scenario characterized by a vanishing transverse local dispersion coefficient, i.e., $\epsilon_2=0$, and a finite longitudinal local dispersion coefficient so that $\epsilon_1=10^{-2}$, which corresponds to $\tau_{D_1}=10^2\tau_u$. For transport in a steady random field, it has been shown [36] that in the absence of transverse local dispersion the effective longitudinal dispersion coefficient is of the order of magnitude of the local dispersion coefficient and the ensemble and effective coefficients do not converge in the limit of infinite times implying that longitudinal local dispersion only is not sufficient to activate advective spreading. The solute is spread out parallel to the mean flow by longitudinal local dispersion and so samples the contrasts of the transverse velocity components. This mechanism, however, is not sufficient to activate macroscopic advective spreading.

For transport in a time-dependent random field the situation is different. Due to the time variation of the flow field, spatial velocity contrasts are amplified and as soon as the solute is spread out sufficiently, i.e., over more than one longitudinal correlation length l_1, advective spreading due to the complicated streamline structure is activated. This can be observed in Fig. 5(a), where we plotted the contributions to the longitudinal dispersion coefficients for $d=2$ dimensions. The behavior for $d=3$ is qualitatively the same and is not displayed here. In the (hypothetical) limit of infinite correlation time, i.e., infinite Kubo number, the contributions due to spatial and temporal fluctuations (scaled by $\sigma_{ff}^2\sigma_{\nu\nu}^2 u l_1$) are formally identical to the contributions due to a steady random velocity field (scaled by $\sigma_{ff}^2 u l_1$). Thus the effective and ensemble coefficients for $\kappa=\infty$, displayed in Figs. 5(a) and 5(b) illustrate the time behavior for transport in a steady random velocity field. The longitudinal effective coefficient for this case is of the order of the local dispersion coefficient and does not cross over to the corresponding ensemble coefficient but approaches a microscopic asymptotic value of the order of the longitudinal local dispersion coefficient. With finite Kubo number the behavior changes. For $\kappa=1$, the effective coefficient evolves to a macroscopic value and converges eventually to the ensemble coefficient.

In the long-time regime for $t \gg \tau_{\kappa_1}$, with $\tau_{\kappa_1} \equiv \tau_{D_1}\kappa^2$, the effective longitudinal coefficient approaches its asymptotic value as

$$\delta^{(t)}\{D_{11}^{\infty}\} - \delta^{(t)}\{D_{11}^{\text{eff}}\} \sim t^{-1/2}. \tag{54}$$

The time scale defining the asymptotic long-time regime is given by τ_{κ_1}, which increases quadratically with κ, and thus, in Fig. 5(a), the effective longitudinal coefficient for $\kappa=1$ converges much faster to its asymptotic value than for $\kappa=10$.

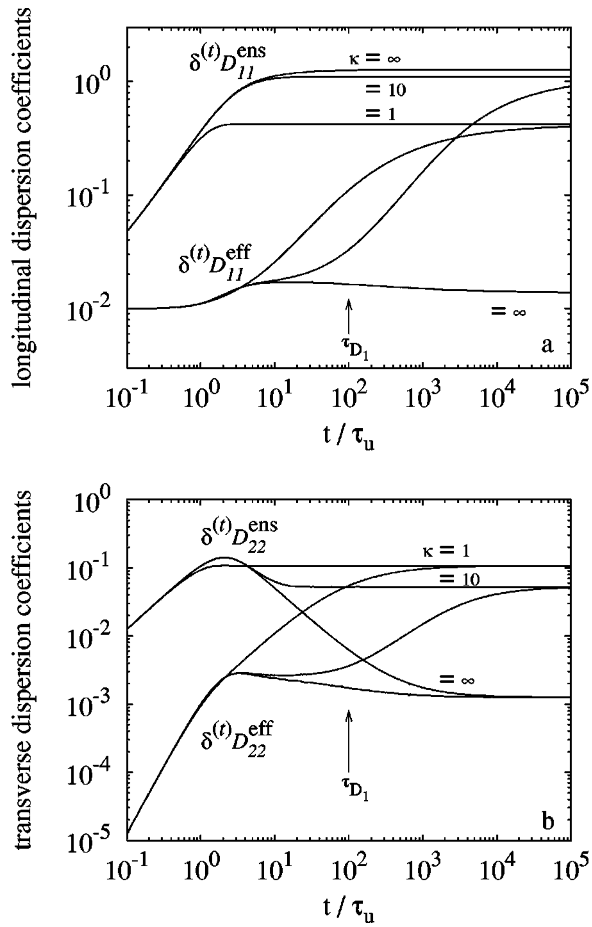

FIG. 5. Time behavior of the contributions to the (a) longitudinal and (b) transverse ensemble and effective dispersion coefficients in $d=2$ dimensions, $\kappa=1,10,\infty$, $\epsilon_2=0$, $\epsilon_1=10^{-2}$.

The behavior of the contributions to the transverse dispersion coefficients is displayed in Fig. 5(b). For infinite Kubo number, which corresponds to the conditions for a steady random field, the effective and ensemble coefficients converge in the long-time limit to a common microscopic asymptotic value. For finite κ, $\delta^{(t)}\{D_{22}^{\text{eff}}\}$ and $\delta^{(t)}\{D_{22}^{\text{ens}}\}$ converge for $t \gg \tau_{\kappa_1}$ to their κ-dependent macroscopic value. The effective coefficients approach the long-time limit algebraically $\sim t^{-d/2}$.

c. Finite longitudinal and transverse local dispersion coefficients. Figures 6(a) and 6(b) illustrate the time behavior of the contributions to the longitudinal and transverse dispersion coefficients, respectively, for varying values of the longitudinal local dispersion coefficient and finite transverse local dispersion in $d=2$.

For $\epsilon_1=0.1$, the effective longitudinal coefficient, Fig. 6(a), evolves algebraically $\sim t^{-1/2}$ in the time regime $\tau_{\kappa_1} \ll t \ll \tau_{D_2}$. This behavior has been already observed in Fig. 5(a) for the case $\epsilon_{22}=0$, where $\tau_{D_2}=\infty$. In this time regime longitudinal local dispersion, enhanced by the temporal fluctuations of the velocity field, represents the only active local transverse spreading mechanism. For $t \gg \tau_{D_2}$, the asymptotic value then is approached in leading order according to $t^{-d/2}$.

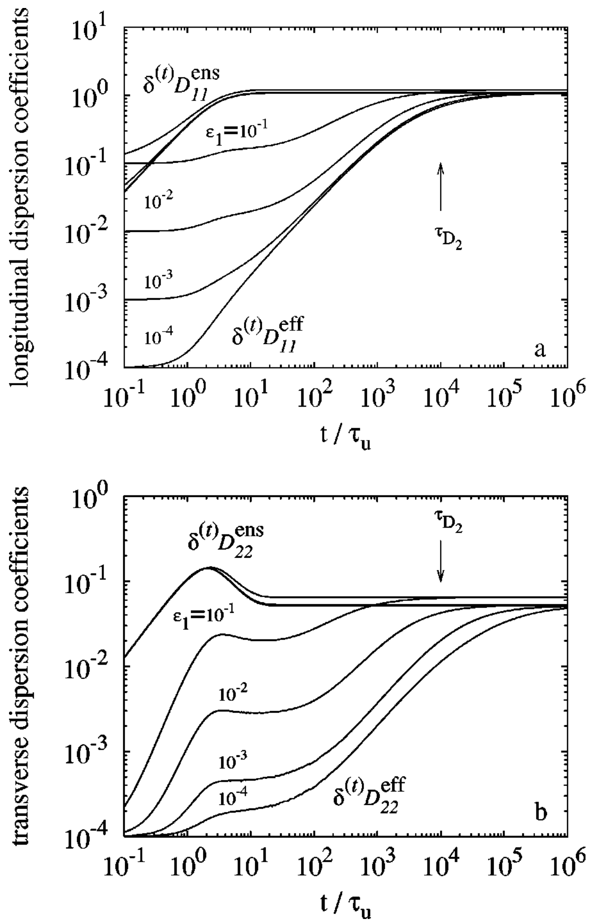

FIG. 6. Time behavior of the contributions to the (a) longitudinal and (b) transverse ensemble and effective dispersion coefficients in $d=2$ dimensions, $\kappa=10$, $\epsilon_2=10^{-4}$, $\epsilon_1=10^{-1}$, 10^{-2}, 10^{-3}, 10^{-4}.

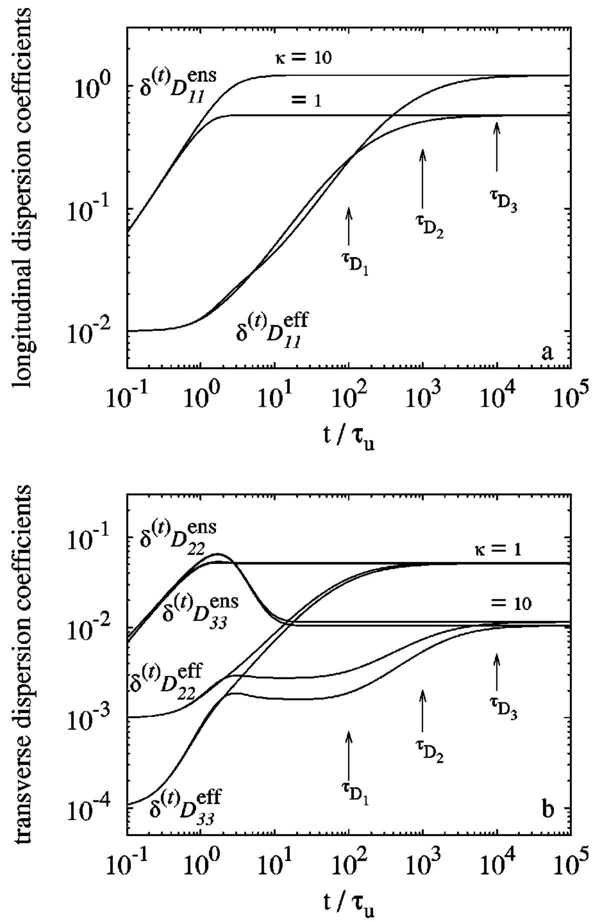

FIG. 7. Time behavior of the contributions to the (a) longitudinal and (b) transverse ensemble and effective dispersion coefficients in $d=3$ dimensions for $\epsilon_1=10^{-2}$, $\epsilon_2=10^{-3}$, and $\epsilon_3=10^{-4}$.

For $\epsilon_1=10^{-2}$, we have $\tau_{\kappa_1}=\tau_{D_2}=10^4\tau_u$. The effective coefficients reach their asymptotic values for $t\gg\tau_{D_2}$ according to t^{-d}.

For decreasing ϵ_1, i.e., increasing τ_{κ_1}, the long-time behavior "saturates" and becomes independent of the longitudinal dispersion time scale. The effective coefficients evolve $\sim t^{-d}$ already for $t\gg\tau_{D_2}$.

The transverse effective coefficients, Fig. 6(b), show the same long-time behavior and evolve asymptotically according to t^{-d}. However, the relevant asymptotic time scale varies with the value of the Kubo number κ. Thus, the effective transverse coefficients evolve on different time scales towards their long-time values, see Fig. 6(b). For $\tau_{\kappa_1}\leq\tau_{D_2}$ the asymptotic regime is defined by $t\gg\tau_{\kappa_1}$, while for $\tau_{\kappa_1}\geq\tau_{D_2}$, τ_{D_2} defines the relevant asymptotic time scale. Thus, for the evolution of the transverse effective coefficients either local dispersion mechanisms together with the temporal fluctuations of the flow velocity is equally efficient to activate macroscopic advective spreading.

Figures 7(a) and 7(b) illustrate the time behavior of the contributions to the longitudinal and transverse dispersion coefficients, respectively, in $d=3$ for $\epsilon_1=10^{-1}$, $\epsilon_2=10^{-3}$, and $\epsilon_3=10^{-4}$. The behavior is similar to the one observed in $d=2$. Here, however, we distinguish three dispersion time scales. The longitudinal effective coefficient for $\kappa=1$, Fig. 7(a), evolves already for $t\gg\tau_{D_1}$ to its asymptotic value, faster than the coefficient for $\kappa=10$ (i.e., $\tau_{\kappa_1}=\tau_{D_3}$), which evolves on τ_{D_2}. Apparently, the second, largest transverse dispersion time scale τ_{D_3} has no remarkable influence on the time evolution of the effective coefficients. The local spreading of the solute due to the local dispersion in the other two directions enhanced by the temporal fluctuations of the flow field is efficient enough to activate the macroscopic spreading due to the complicated streamline structure already for $t\gg\tau_{D_3}$. This behavior is different from that observed in steady random flow, where the time behavior changes quantitatively for $t\gg\tau_{D_3}$ [36].

The transverse effective dispersion coefficients for $\kappa=1$, Fig. 7(b), increase monotonously towards the asymptotic value, which they approach for $t\gg\tau_{D_1}$. The transverse dispersion scales have no remarkable effect on the asymptotic behavior. For $\kappa=10$ (i.e., $\tau_{\kappa_1}=\tau_{D_3}$) the behavior of the effective coefficients is nonmonotonic for $t/\tau_u\leq\kappa$. However, the behavior in this time regime has only a formal meaning because the stochastic approach cannot be assumed to be valid for such times due to large sample to sample fluctuations of the temporal stochastic process. For $t/\tau_u > \kappa$ the transverse effective coefficients cross over towards their macroscopic asymptotic values, which they approach for $t \gg \tau_{D_2}$. Again, the much larger time scales τ_{D_3} and τ_{κ_1} play only a minor role for the time evolution of the effective coefficients. Longitudinal local dispersion is effective only due to the interplay with the time fluctuations of the velocity field.

IV. SUMMARY

We investigated the effective transport behavior of a passive solute evolving from a point-like injection in the incompressible flow through a heterogeneous porous medium subject to temporal fluctuations of the boundary conditions of the flow equation. We used a stochastic approach to analyze the interplay of local scale spatial heterogeneities, local dispersion, and temporal fluctuations of the flow field and its effect on the large scale transport behavior. In this approach the medium heterogeneities are represented by a spatial random process while the fluctuations of the boundary conditions are modeled as a temporal random field with finite correlation time. The incompressible velocity field for flow in a heterogeneous porous medium is given by the Darcy equation, which is solved by perturbation theory in the fluctuations of the random fields. The obtained perturbation solution consists of three contributions: (1) A spatially constant, time-dependent part, (2) a temporally constant, spatially fluctuating part, and (3) a space- and time-dependent contribution. We focused on the transport relevant contributions due to the third term whereby we took into account only temporal variations of the magnitude of the spatial mean velocity. The effect of the second term on the large scale transport behavior is already well investigated in the stochastic perturbative framework. It turned out that the first, only temporally varying contribution has no influence on the effective spreading of the solute.

In the stochastic approach, the observables are defined as averages over all typical realizations of the underlying random fields and have to be carefully chosen in order to represent the actual spreading in a typical realization of the heterogeneous medium. In analogy to transport in a steady random flow field, we defined the effective dispersion coefficient D_{ij}^{eff} (18), which characterizes the spreading in a typical disorder realization. The conceptually different ensemble dispersion coefficient D_{ij}^{ens} (19) quantifies the artificial spreading due to the sample to sample fluctuations of the center of mass velocity. Both dispersion coefficients converge on sufficiently large scales (set by the local dispersion), where the advective macroscale spreading becomes a real effect as a consequence of transverse spreading due to local dispersion and the interaction with temporal fluctuations of the flow field.

Other definitions for the large scale dispersion coefficients, which are derived from the time ensemble averaged concentration distribution (e.g., Refs. [5,10]) have been shown to be inappropriate for the characterization of solute spreading in a typical heterogeneity realization: We studied the exactly solvable case of transport in a time-dependent flow through a homogeneous medium. There, the concentration distribution in one realization is given by a Gaussian function characterized by the (constant) local dispersion and the time-dependent center of mass velocity, which is identical to the flow velocity. For a Gaussian distributed random flow field, the ensemble averaged concentration was determined explicitly. The "macrodispersion" coefficients derived from this averaged concentration are given in terms of the temporal correlation of the flow field and are for all times quantitatively different from the local dispersion coefficients, which measure the spreading in a typical realization. These "macrodispersion" coefficients are not self-averaging and as such are not representative of the spreading in a typical disorder realization. Thus, in order to study the effective transport behavior in transient flow through a heterogeneous medium we focused on the effective and ensemble dispersion coefficients.

The complete time evolution of the large scale dispersion coefficients was investigated by numerical and analytical evaluation of the resulting second-order perturbation theory expressions. It was found that the transport behavior in a time-dependent heterogeneous flow field is qualitatively similar, quantitatively different, though, from the one observed in steady random flow. The stochastic perturbative analysis of transport in a steady flow field yields transverse asymptotic dispersion coefficients of the order of the (microscopic) local dispersion coefficient and is in contradiction to experimental findings. In a temporally fluctuating heterogeneous flow field, however, the contributions to the longitudinal and transverse effective dispersion coefficients evolve on sufficiently large scales to (constant) macroscopic long-time values. Apparently, the interaction between local scale dispersion and time fluctuations of the flow velocity enhance the mixing of the solute and so activate advective spreading due to the complicated streamline structure.

In the long-time limit $t \to \infty$ the ensemble and effective dispersion coefficients converge to the same asymptotic values. Both the contributions to the longitudinal as well as to the transverse asymptotic dispersion coefficients are of macroscopic order of magnitude, which is consistent with field observations. The longitudinal asymptotic values increase monotonically with increasing Kubo number $\kappa = \tau/\tau_u$, which measures the correlation time scale in units of the advection time scale. In the (hypothetical) limit $\kappa \to \infty$ it tends to a macroscopic asymptotic value $\sim \kappa^{-(d-1)}$. The transverse asymptotic contributions assume a maximum for $\kappa \approx 1$, and decrease in the hypothetical case of $\kappa \to \infty$ according to $\sim \kappa^{-(d-1)}$ to a value of the order of the local dispersion coefficient. For κ around 1, the ratio between the transverse and longitudinal contributions is of the order of magnitude of the ratio usually adopted by hydrologists.

The longitudinal and transverse ensemble quantities evolve on the correlation time scale exponentially to their asymptotic value. The effective coefficients evolve on time scales set by the local dispersion coefficients and the Kubo number $\kappa = \tau/\tau_u$. For large Kubo numbers, the longitudinal effective coefficients evolve in an intermediate time regime $\tau_D \ll t \ll \tau_\kappa$ as $\sim t^{-(d-1)/2}$ like in a steady random flow. The time scale $\tau_\kappa = l_\kappa^2/D$, with $l_\kappa = u\tau$, characterizes the time for the local dispersive spreading of the solute over the distance which the solute is transported advectively during one correlation time. As such it characterizes the time after which the interplay between temporal fluctuations and local dispersion becomes effective as an additional transverse local spreading mechanism. Then, for $t \gg \tau_\kappa$ due to the influence of time fluctuations of the flow velocity, the effective coefficients evolve faster than for steady random flow according to $\sim t^{-d/2}$. The transverse effective coefficients evolve for $t \gg \tau_\kappa$ in the same way. The same long-time behavior is observed for transport with zero local longitudinal dispersion.

For vanishing transverse local dispersion, however, the behavior is different. In this case the effective longitudinal coefficient approaches its macroscopic asymptotic value algebraically $\sim t^{-1/2}$ for $t \gg \tau_{\kappa_1}$, with $\tau_{\kappa_1} = l_\kappa^2/D_1$. An intermediate time regime for $\kappa \gg 1$ is not observable. In a steady random flow the effective longitudinal coefficient evolves to a macroscopic value solely due to the transverse mixing induced by local transverse dispersion. Thus, for zero transverse local dispersion it remains of the order of the local dispersion coefficient. By longitudinal local dispersion, the solute experiences the contrasts of the transverse velocity components along the 1-direction, which, however, is not sufficient to activate advective spreading in steady random flows. Temporal fluctuations enhance these velocity contrasts and lead to the observed macroscale advective spreading.

The results presented in this paper are inherently perturbative, i.e., strictly valid only for moderate fluctuations of the medium properties and the boundary conditions of the flow equations. It is not clear up to which variances of the random fields this approach is valid. The application of nonperturbative solution methods and the comparison to numerical simulations can give further insights into this important questions. In fact, the comparison to numerical Monte Carlo simulations [42] indicates that the presented results are still valid for an increasing variance of the random flow field. Work along this line is in progress.

The local dispersion tensor has been set constant in this study. In general, however, it is also dependent on the locally fluctuating flow velocity [43]. Moreover, in field experiments it is observed, e.g., Refs. [4–6], that not only the magnitude but also the direction of the spatial mean flow velocity $\mathbf{u}(t) = \overline{\mathbf{u}(\mathbf{x},t)}$ varies with time. The method used in this paper allows for a systematic analysis of these cases as well as for the investigation of the influence of extended initial conditions on the macroscale transport behavior, which is important for the comparison to field scale experiments. Furthermore, the consequences of these results for remediation techniques, which rely on the mixing of injected reactants with contaminated ground water [44], have to be explored.

ACKNOWLEDGMENTS

The financial support of the Spanish Secretaría de Estado de Educación y Universidades and the European Commission (Contract No. EVK1-CT-2000-00062) is gratefully acknowledged.

APPENDIX A: LINEARIZED SOLUTION OF THE DARCY EQUATION

The following perturbative solution of the Darcy equation follows the derivation given in Refs. [2,5]. The Darcy equation represents an effective flow law on a mesoscopic length scale and relates the flow velocity $\mathbf{u}(\mathbf{x},t)$ in the porous medium to the hydraulic gradient $\nabla h(\mathbf{x},t)$, where $h(\mathbf{x},t)$ denotes the hydraulic head, e.g., Ref. [24]:

$$\mathbf{u}(\mathbf{x},t) = -\exp[f(\mathbf{x})]\nabla h(\mathbf{x},t) \tag{A1}$$

with $f(\mathbf{x})$ being the log-hydraulic conductivity. In the stochastic framework, $f(\mathbf{x})$ is assumed to be a stationary Gaussian distributed spatial random function characterized by the mean value $\overline{f(\mathbf{x})} = \overline{f}$ and its autocorrelation function $\overline{f'(\mathbf{x})f'(\mathbf{x}')} = C^{ff}(\mathbf{x}-\mathbf{x}')$, where $f'(\mathbf{x})$ denotes the fluctuations about the mean value, $f(\mathbf{x}) = \overline{f} - f'(\mathbf{x})$. The mean of $f'(\mathbf{x})$ vanishes by definition. Neglecting compressibility of fluid and solid matrix, mass conservation implies $\nabla \cdot \mathbf{u}(\mathbf{x},t) = 0$, which can be rewritten using Eq. (A1) as an equation for the hydraulic head:

$$\Delta h(\mathbf{x},t) - \nabla f'(\mathbf{x}) \cdot \nabla h(\mathbf{x},t) = 0. \tag{A2}$$

We assume that the boundary conditions for the hydraulic head lead to a temporally fluctuating space independent hydraulic gradient in the absence of spatial fluctuations of the hydraulic conductivity, i.e., $f'(\mathbf{x}) \equiv 0$. The realization of such boundary conditions is outlined in Ref. [8]. The head solution for the homogeneous flow problem, $h_0(\mathbf{x},t)$, then is a linear function of the coordinates so that the hydraulic gradient

$$\mathbf{J}(t) \equiv \nabla h_0(\mathbf{x},t). \tag{A3}$$

We separate the solution $h(\mathbf{x},t)$ into $h_0(\mathbf{x},t)$ and spatial random fluctuations about it, which vanish in the case $f'(\mathbf{x}) \equiv 0$,

$$h(\mathbf{x},t) = h_0(\mathbf{x},t) - h'(\mathbf{x},t). \tag{A4}$$

By inserting this expression into Eq. (A2), we obtain for $h'(\mathbf{x})$,

$$\Delta h'(\mathbf{x},t) - \nabla f'(\mathbf{x}) \cdot \nabla h'(\mathbf{x},t) = \mathbf{J}(t) \cdot \nabla f'(\mathbf{x}), \tag{A5}$$

where $h'(\mathbf{x},t)$ vanishes on the boundaries by definition. The integral equation equivalent to Eq. (A5) reads

$$h'(\mathbf{x},t) = \int_\Omega d^d x' \, \varphi_0(\mathbf{x},\mathbf{x}')[\nabla' f'(\mathbf{x}') \cdot \nabla' h'(\mathbf{x}',t) + \mathbf{J}(t) \cdot \nabla' f'(\mathbf{x}')], \tag{A6}$$

where Ω denotes the flow domain, ∇' denotes the gradient with respect to $\mathbf{x}'$. The Green function $\varphi_0(\mathbf{x},\mathbf{x}')$ solves

$$\Delta \varphi_0(\mathbf{x},\mathbf{x}') = \delta(\mathbf{x}-\mathbf{x}'), \tag{A7}$$

where $\varphi_0(\mathbf{x},\mathbf{x}')$ vanishes on the boundaries. We want to determine the flow field far away from the boundaries. Thus, we now consider the limiting case of an infinite flow domain. For convenience we perform a spatial Fourier transform. The spatial Fourier transform of the integral equation (A6) is given by

$$\tilde{h}'(\mathbf{k},t)=\frac{i\mathbf{k}\cdot\mathbf{J}(t)}{k^2}\tilde{f}'(\mathbf{k})-\frac{i}{k^2}\int_{k'}(\mathbf{k}-\mathbf{k}')\cdot\mathbf{k}'\tilde{f}'(\mathbf{k}')\tilde{h}'(\mathbf{k}',t), \tag{A8}$$

because the Green function $\varphi_0(\mathbf{x},\mathbf{x}')$ in Fourier space reads (e.g., Ref. [45])

$$\tilde{\varphi}_0(\mathbf{k},\mathbf{k}')=\frac{1}{k^2}(2\pi)^d\delta(\mathbf{k}+\mathbf{k}'). \tag{A9}$$

Iterating Eq. (A8) one obtains a perturbation series for $\tilde{h}'(\mathbf{k},t)$. We truncate after the first-order term in $\tilde{f}'(\mathbf{k})$, i.e., we take into account only the first term of the right side of Eq. (A8). We then insert this expression into Eq. (A1). We expand the resulting expression consistently up to first order in $\tilde{f}'(\mathbf{k})$ and obtain for the flow velocity:

$$u_i(\mathbf{x},t)=K_gJ_i(t)-K_g\int_k\exp(-i\mathbf{k}\cdot\mathbf{x})\times\left(J_i(t)-\frac{k_i\mathbf{k}\cdot\mathbf{J}(t)}{k^2}\right)\tilde{f}'(\mathbf{k})+\cdots, \tag{A10}$$

where $K_g\equiv\exp(\overline{f})$. Starting from this expression, we consider the temporal fluctuations of spatial mean hydraulic gradient $\mathbf{J}(t)$. The time stochastic process is assumed to be stationary so that the mean gradient $\langle\mathbf{J}(t)\rangle\equiv\mathbf{J}$ is time independent. We consider here transport situations where the mean hydraulic gradient is parallel to the mean flow velocity, i.e., mean flow parallel to the bedding, e.g., Ref. [2]. Thus, without loss of generality, we assume $\mathbf{J}$ to be aligned with the one direction of the coordinate system. The results derived here can be generalized straightforwardly to the case of complete anisotropy. We now divide $\mathbf{J}(t)$ into its mean value and fluctuations about it,

$$J_i(t)=J(\delta_{i1}-\nu_i(t)), \tag{A11}$$

$i=1,\dots,d$, where the $\nu_i(t)$ denotes the normalized fluctuations about $\langle J_i(t)\rangle$. Inserting Eq. (A11) into Eq. (A10) we obtain contributions (6)–(8) of decomposition (5) of the flow field in terms of the perturbative mean velocity $u\equiv K_gJ$. Using a flow factor γ [2] u can be written in the form of the experimentally accessible (nonperturbative) mean velocity $u^{\exp}$, $u=u^{\exp}\gamma^{-1}$. The flow factor is defined by $\gamma=K_{11}/K_g$ with K_{11} the experimentally given 11-coefficient of the macroscopic hydraulic conductivity. (If the flux is prescribed at the inflow boundary the flow factor drops since the mean flow is imposed by the boundary condition. For the perturbative solution of this boundary value problem, one considers an equation for the vector potential of the incompressible flow, $\mathbf{A}(\mathbf{x},t)$ with $\mathbf{u}(\mathbf{x},t)=\nabla\times\mathbf{A}(\mathbf{x},t)$, instead of the scalar potential $h(\mathbf{x},t)$, see Ref. [46].)

APPENDIX B: SOLUTIONS

1. Asymptotic behavior

Here we present analytical solutions for the asymptotic behavior of the longitudinal and transverse macrodispersion coefficients as a function of the Kubo number $\kappa\equiv\tau/\tau_u$ for isotropic spatial disorder and an isotropic local dispersion tensor. For vanishing local dispersion and isotropic disorder correlation, we obtain for the asymptotic longitudinal and transverse dispersion coefficients as a function of κ in $d=3$ dimensions:

$$\delta^{(t)}\{D_L^\infty\}(\kappa)=\sigma_{ff}^2\sigma_{\nu\nu}^2ul\sqrt{\frac{\pi}{2}}\kappa^{-4}\left\{\left(\kappa^2+\frac{3}{4}\right)\times\ln\left(\frac{-\kappa+\sqrt{1+\kappa^2}}{\kappa+\sqrt{1+\kappa^2}}\right)+\sqrt{1+\kappa^2}\left(\kappa^3+\frac{3}{2}\kappa\right)\right\}, \tag{B1}$$

$$\delta^{(t)}\{D_T^\infty\}(\kappa)=\sigma_{ff}^2\sigma_{\nu\nu}^2ul\frac{\sqrt{\pi}}{16\kappa^4}\left\{(2\sqrt{2}\kappa^2+3\sqrt{2})\times\ln\left(\frac{\kappa+\sqrt{1+\kappa^2}}{-\kappa+\sqrt{1+\kappa^2}}\right)-6\sqrt{2}\kappa\sqrt{1+\kappa^2}\right\}. \tag{B2}$$

The maximum of $\delta^{(t)}\{D_T^\infty\}(\kappa)$ is reached for $\kappa\approx1$, i.e., at correlation times of the order of the advection time scale τ_u. In $d=2$ dimensions we obtain

$$\delta^{(t)}\{D_L^\infty\}(\kappa)=\sigma_{ff}^2\sigma_{\nu\nu}^2ul\sqrt{\frac{\pi}{2}}\kappa^{-3}\left\{(1+\kappa^2)^{3/2}-\frac{3}{2}\kappa^2-1\right\}, \tag{B3}$$

$$\delta^{(t)}\{D_T^\infty\}(\kappa)=\sigma_{ff}^2\sigma_{\nu\nu}^2ul\sqrt{\frac{\pi}{2}}\kappa^{-3}\left\{\frac{1}{2}\kappa^2-\sqrt{1+\kappa^2}+1\right\}. \tag{B4}$$

The maximum of $\delta^{(t)}\{D_T^\infty\}(\kappa)$ in $d=2$ is given by $\delta^{(t)}\{D_T^\infty\}(\kappa_{\max})=\frac{1}{6}\sqrt{\pi/6}\sigma_{ff}^2\sigma_{\nu\nu}^2ul$, and reached at $\kappa_{\max}=\sqrt{3}$.

2. Time behavior

The time behavior of the ensemble and effective dispersion coefficients is determined by the numerical evaluation of the auxiliary functions (41), which in $d=3$ dimensions can be simplified to

$$M_{11}(t,\mathbf{A})=\sigma_{\nu\nu}^2\sigma_{ff}^2\frac{\sqrt{2}l_2l_3}{4l_1^2}\int_0^{t/\tau_u}dt'\int_0^1 dx B_1(t',\mathbf{A})^{3/2}x^2 \times(1-x^2)\exp\left(-\frac{(xt')^2}{4B_1(t',\mathbf{A})}-\frac{t'^2}{2\kappa^2}\right) \times\{3/2[B_1(t',\mathbf{A})+\Delta B_2(t',\mathbf{A})x^2]^{-1/2}[B_1(t',\mathbf{A}) +\Delta B_3(t',\mathbf{A})x^2]^{-5/2}+[B_1(t',\mathbf{A}) +\Delta B_2(t',\mathbf{A})x^2]^{-5/2}[B_1(t',\mathbf{A}) +\Delta B_3(t',\mathbf{A})x^2]^{-1/2}+[B_1(t',\mathbf{A}) +\Delta B_2(t',\mathbf{A})x^2]^{-3/2}[B_1(t',\mathbf{A}) +\Delta B_3(t',\mathbf{A})x^2]^{-3/2}\}, \tag{B5}$$

$$M_{22}(t,\mathbf{A})=\sigma_{\nu\nu}^2\sigma_{ff}^2\frac{\sqrt{2}l_2l_3}{8l_1^2}\int_0^{t/\tau_u}dt'\int_0^1 dx(1-x^2) \times\exp\left(-\frac{(xt')^2}{4B_1(t',\mathbf{A})}-\frac{t'^2}{2\kappa^2}\right)\left(B_1(t',\mathbf{A})^{1/2}x^2 -\frac{1}{2}B_1(t',\mathbf{A})^{-1/2}t'^2x^4\right)[B_1(t',\mathbf{A}) +\Delta B_2(t',\mathbf{A})x^2]^{-3/2}[B_1(t',\mathbf{A}) +\Delta B_3(t',\mathbf{A})x^2]^{-1/2}, \tag{B6}$$

$$M_{33}(t,\mathbf{A})=\sigma_{\nu\nu}^2\sigma_{ff}^2\frac{\sqrt{2}l_2l_3}{8l_1^2}\int_0^{t/\tau_u}dt'\int_0^1 dx(1-x^2) \times\exp\left(-\frac{(xt')^2}{4B_1(t',\mathbf{A})}-\frac{t'^2}{2\kappa^2}\right)\left(B_1(t',\mathbf{A})^{1/2}x^2 -\frac{1}{2}B_1(t',\mathbf{A})^{-1/2}t'^2x^4\right)[B_1(t',\mathbf{A}) +\Delta B_3(t',\mathbf{A})x^2]^{-3/2}[B_1(t',\mathbf{A}) +\Delta B_2(t',\mathbf{A})x^2]^{-1/2}, \tag{B7}$$

where we defined for compactness of notation:

$$B_i(t,\mathbf{A})=\frac{1}{2}(A_i\pm 2\epsilon_i t), \tag{B8}$$

$$\Delta B_j(t,\mathbf{A})=l_j^2/l_1^2B_j(t,\mathbf{A})-B_1(t,\mathbf{A}), \quad j\neq 1. \tag{B9}$$

In $d=2$ dimensions, we obtain

$$M_{ii}(t,\mathbf{A})=\sigma_{\nu\nu}^2\sigma_{ff}^2\frac{l_2}{l_1\pi}\int_0^{t/\tau_u}dt'\int_0^1 dx B(x,t',\mathbf{A})^{-1} \times\exp\left(-\frac{t'^2}{2\kappa^2}\right)\left[1-\frac{xt'}{B(x,t',\mathbf{A})^{1/2}} \times\mathcal{D}\left(\frac{xt'}{2\sqrt{B(x,t',\mathbf{A})}}\right)\right]h_i(x), \tag{B10}$$

where the function $\mathcal{D}(x)$ denotes Dawson's integral as defined in Ref. [47]. We defined for compactness of notation:

$$h_i(x)=\begin{cases}(1-x^2)^{3/2}, & i=1\\ x^2(1-x^2)^{1/2}, & i=2\end{cases} \tag{B11}$$

and

$$B(x,t,\mathbf{A})=\frac{1}{2}[(A_1\pm 2\epsilon_1 t^2)x^2+l_2^2/l_1^2(A_2\pm 2\epsilon_2 t^2)(1-x^2)]. \tag{B12}$$

a. Approximation for small inverse Peclet numbers and $t\gg\tau_u$

For isotropic spatial disorder, $l_1=\cdots=l_d$, the auxiliary functions (41) can be evaluated explicitly for $\epsilon_l\ll 1$, $l=1,\cdots,d$, and $t\gg\tau_u$. We consider a situation with isotropic disorder correlation $l_1=\cdots=l_d$ and anisotropic local dispersion with $D_{11}=D_L$ and $D_{ii}=D_T$, $i\neq 1$. Therefore we define for $d=2$ and $d=3$ dimensions, $M_1^\pm\equiv M_L^\pm$, and $M_i^\pm\equiv M_T^\pm$ for $i\neq 1$ and $A_1\equiv A_L$, $A_i\equiv A_T$ for $i\neq 1$. The approximate behavior is obtained by setting $\epsilon_l=0$ in Eq. (41) and extending the upper bound of the time integration to infinity [36]. This yields for $d=3$ dimensions:

$$M_L^\pm(t,\mathbf{A})=\sqrt{\frac{\pi}{2}}\sigma_{\nu\nu}^2\sigma_{ff}^2\left[\frac{\kappa}{\sqrt{A_L+\kappa^2}}\left(\frac{1}{A_T}+\frac{5}{2(\Delta A+\kappa^2)} +\frac{3A_T}{2(\Delta A+\kappa^2)^2}\right) -\frac{\kappa}{(\Delta A+\kappa^2)^{3/2}}\mathrm{arcsinh}\left(\sqrt{\frac{(\Delta A+\kappa^2)}{A_T}}\right) \times\left(\frac{3A_T}{2(\Delta A+\kappa^2)}+2\right)\right], \tag{B13}$$

$$M_T^{\pm}(t,\mathbf{A}) = \sqrt{\frac{\pi}{2}}\sigma_{\nu\nu}^2\sigma_{ff}^2\left[\frac{\kappa}{(\Delta A+\kappa^2)^{3/2}}\operatorname{arcsinh}\left(\sqrt{\frac{(\Delta A+\kappa^2)}{A_T}}\right)\times\left(\frac{3A_T}{4(\Delta A+\kappa^2)}+\frac{1}{2}\right)-\frac{\kappa}{\sqrt{A_L+\kappa^2}}\left(\frac{3}{4(\Delta A+\kappa^2)}+\frac{3A_T}{4(\Delta A+\kappa^2)^2}\right)\right]. \tag{B14}$$

In $d=2$ dimensions, we obtain

$$M_L^{\pm}(t,\mathbf{A}) = \sqrt{\frac{\pi}{2}}\sigma_{\nu\nu}^2\sigma_{ff}^2\left[\frac{1}{\sqrt{A_T}}\frac{\kappa(A_L+\kappa^2)^{3/2}}{(\Delta A+\kappa^2)^2}-\frac{\kappa}{\Delta A+\kappa^2}\left(\frac{A_T}{\Delta A+\kappa^2}+\frac{3}{2}\right)\right], \tag{B15}$$

$$M_T^{\pm}(t,\mathbf{A}) = \sqrt{\frac{\pi}{2}}\sigma_{\nu\nu}^2\sigma_{ff}^2\left[\frac{\kappa}{\Delta A+\kappa^2}\left(\frac{A_T}{\Delta A+\kappa^2}+\frac{1}{2}\right)-\frac{\kappa\sqrt{A_T}(A_L+\kappa^2)^{1/2}}{(\Delta A+\kappa^2)^2}\right], \tag{B16}$$

where for compactness of notation we defined $\Delta A \equiv A_L - A_T$. For isotropic local dispersion $\Delta A \equiv 0$. Note that the $M_{ii}^{\pm}$ have no explicit time dependence but vary only if $\mathbf{A}$ is time-dependent.

b. Closed expressions in d=2 spatial dimensions for the limiting case of zero local dispersion

For the contributions to the longitudinal and transverse dispersion coefficients we obtain explicit expressions in $d=2$ spatial dimensions in the limiting case of vanishing local dispersion $D=0$ and isotropic disorder correlation $l_1=\cdots=l_d=l$. We define here the dimensionless time $\hat{t}\equiv t/\tau_u$. For the time behavior of $\delta^{(t)}\{D_{11}^{\text{ens}}(t)\}$ we obtain from the $M_{ii}^{\pm}$, Eq. (48) according to Eqs. (43) and (44):

$$\delta^{(t)}\{D_{11}^{\text{ens}}(t)\} = \sigma_{\nu\nu}^2\sigma_{ff}^2 ul\left[\sqrt{\frac{\pi}{2}}\frac{\operatorname{erf}\left(\frac{t}{\sqrt{2}\tau}\sqrt{1+\kappa^2}\right)}{\sqrt{1+\kappa^2}}\times\{\kappa^{-1}+2\kappa^{-3}+\kappa^{-5}\}-\sqrt{\frac{\pi}{2}}\operatorname{erf}\left(\frac{t}{\sqrt{2}\tau}\right)\times\left\{\frac{3}{2}\kappa^{-1}+\kappa^{-3}\right\}+\exp\left(-\frac{t^2}{2\tau^2}(1+\kappa^2)\right)\times\{\hat{t}^{-1}+\hat{t}^{-1}\kappa^{-2}-\hat{t}^{-3}\}+\exp\left(-\frac{t^2}{2\tau^2}\right)\times\left\{\hat{t}^{-3}-\hat{t}^{-1}\kappa^{-2}-\frac{3}{2}\hat{t}^{-1}\right\}\right]. \tag{B17}$$

For the time behavior of $\delta^{(t)}\{D_{22}^{\text{ens}}(t)\}$ we obtain

$$\delta^{(t)}\{D_{22}^{\text{ens}}(t)\} = \sigma_{\nu\nu}^2\sigma_{ff}^2 ul\left[-\sqrt{\frac{\pi}{2}}\frac{\operatorname{erf}\left(\frac{t}{\sqrt{2}\tau}\sqrt{1+\kappa^2}\right)}{\sqrt{1+\kappa^2}}\times\{\kappa^{-3}+\kappa^{-5}\}+\sqrt{\frac{\pi}{2}}\operatorname{erf}\left(\frac{t}{\sqrt{2}\tau}\right)\times\left\{\frac{1}{2}\kappa^{-1}+\kappa^{-3}\right\}+\exp\left(-\frac{t^2}{2\tau^2}(1+\kappa^2)\right)\times\{\hat{t}^{-3}-\hat{t}^{-1}\kappa^{-2}\}+\exp\left(-\frac{t^2}{2\tau^2}\right)\times\left\{\frac{1}{2}\hat{t}^{-1}+\hat{t}^{-1}\kappa^{-2}-\hat{t}^{-3}\right\}\right]. \tag{B18}$$

[1] G. Dagan, *Flow and Transport in Porous Formations* (Springer, New York, 1989).
[2] L.W. Gelhar and C. Axness, Water Resour. Res. **19**, 161 (1983).
[3] L.W. Gelhar, *Stochastic Subsurface Hydrology* (Prentice-Hall, Englewood Cliffs, NJ, 1993).
[4] D.L. Freyberg, Water Resour. Res. **22**, 2031 (1986).
[5] K.R. Rehfeldt and L.W. Gelhar, Water Resour. Res. **28**, 2085 (1992).
[6] E.A. Sudicky, Water Resour. Res. **22**, 2069 (1986).
[7] P. Ackerer and W. Kinzelbach (unpublished).
[8] D.J. Goode and L.F. Konikow, Water Resour. Res. **10**, 2339 (1990).
[9] B.D. Wood and M.L. Kavvas, Water Resour. Res. **7**, 2053 (1999).
[10] M. Shvidler and K. Karasaki, Transp. Porous Media **50**, 223 (2003).
[11] O. Cirpka, Geophys. Res. Abstracts **5**, 01 501 (2003).
[12] J.A. Aronovitz and D.R. Nelson, Phys. Rev. A **30**, 1948 (1984).
[13] J.-P. Bouchaud and A. Georges, Phys. Rep. **195**, 127 (1990).
[14] M.W. Deem, Phys. Rev. E **51**, 4319 (1995).
[15] D.S. Dean, I.T. Drummond, and R.R. Horgan, Phys. Rev. E **63**, 061205 (2001).
[16] I.T. Drummond, S. Duane, and R.R. Horgan, J. Fluid Mech.

138, 75 (1984).
[17] D.S. Fisher, D. Friedan, Z. Qiu, S.J. Shenker, and S.H. Shenker, Phys. Rev. A **31**, 3841 (1985).
[18] U. Frisch, *Turbulence* (Cambridge University Press, 1995).
[19] T. Komorowski and S. Olla, J. Stat. Phys. **108**, 647 (2002).
[20] R.H. Kraichnan, Phys. Fluids **13**, 22 (1970).
[21] R.H. Kraichnan, J. Fluid Mech. **77**, 753 (1976).
[22] R. Reigada, A.C. Marti, I.M. Sokolov, F. Sagues, and J.M. Sancho, Phys. Rev. E **62**, 4997 (2000).
[23] M. Vlad, F. Spineanu, J.H. Misguich, and R. Balescu, Phys. Rev. E **63**, 066304 (2001).
[24] J. Bear, *Dynamics of Fluids in Porous Media* (American Elsevier, New York, 1972).
[25] J.P. Gleeson, Phys. Rev. E **66**, 038301 (2002).
[26] M. Vlad, F. Spineanu, J.H. Misguich, and R. Balescu, Phys. Rev. E **66**, 038302 (2002).
[27] *Stochastic Modelling in Physical Oceanography*, edited by R. J. Adler, P. Müller, and B.L. Rozovskii (Birkhäuser, Boston, 1995).
[28] M.B. Isichenko, Rev. Mod. Phys. **64**, 961 (1992).
[29] W.D. McComb, *The Physics of Fluid Turbulence* (Clarendon, Oxford, 1990).
[30] G.K. Batchelor, Aust. J. Sci. Res. **2**, 437 (1949).
[31] G.K. Batchelor, Proc. Cambridge Philos. Soc. **48**, 345 (1952).
[32] P.K. Kitanidis, J. Hydrol. **102**, 453 (1988).
[33] O. Cirpka and P. Kitanidis, Water Resour. Res. **36**, 1221 (2000).
[34] O. Cirpka, J. Contam. Hydrol. **58**, 261 (2002).
[35] S. Attinger, M. Dentz, H. Kinzelbach, and W. Kinzelbach, J. Fluid Mech. **386**, 77 (1999).
[36] M. Dentz, H. Kinzelbach, S. Attinger, and W. Kinzelbach, Water Resour. Res. **36**, 3591 (2000).
[37] H. Rajaram and L.W. Gelhar, Water Resour. Res. **29**, 3249 (1993).
[38] M. Dentz, H. Kinzelbach, S. Attinger, and W. Kinzelbach, Water Resour. Res. **38**(7), 23-1 (2002).
[39] M. Dentz, H. Kinzelbach, S. Attinger, and W. Kinzelbach, Phys. Rev. E **67**, 046306 (2003).
[40] S. Attinger, M. Dentz, and W. Kinzelbach, Stochastic Environ. Res. Risk. Assess. (to be published).
[41] C.W. Fetter, *Contaminant Hydrogeology* (Prentice-Hall, Englewood Cliffs, NJ, 1998).
[42] Dentz and Carrera (unpublished).
[43] A.E. Scheidegger, J. Geophys. Res. **66**, 3273 (1961).
[44] I. Jones, D.N. Lerner, and S.F. Thornton, in Proceedings of the Groundwater Quality 2001 Conference, Sheffield, UK, 2001, edited by Steven F. Thornton and Sascha E. Oswald, IAHS Publication No. 275 (unpublished).
[45] H.S. Carslaw and J.C. Jaeger, *Conduction of Heat in Solids* (Oxford University Press, New York, 1993).
[46] M. Dentz, Doctoral dissertation, Ruperto-Carola University of Heidelberg, 2000.
[47] M. Abramowitz and I.A. Stegun, *Handbook of Mathematical Functions* (Dover Publications, New York, 1972).